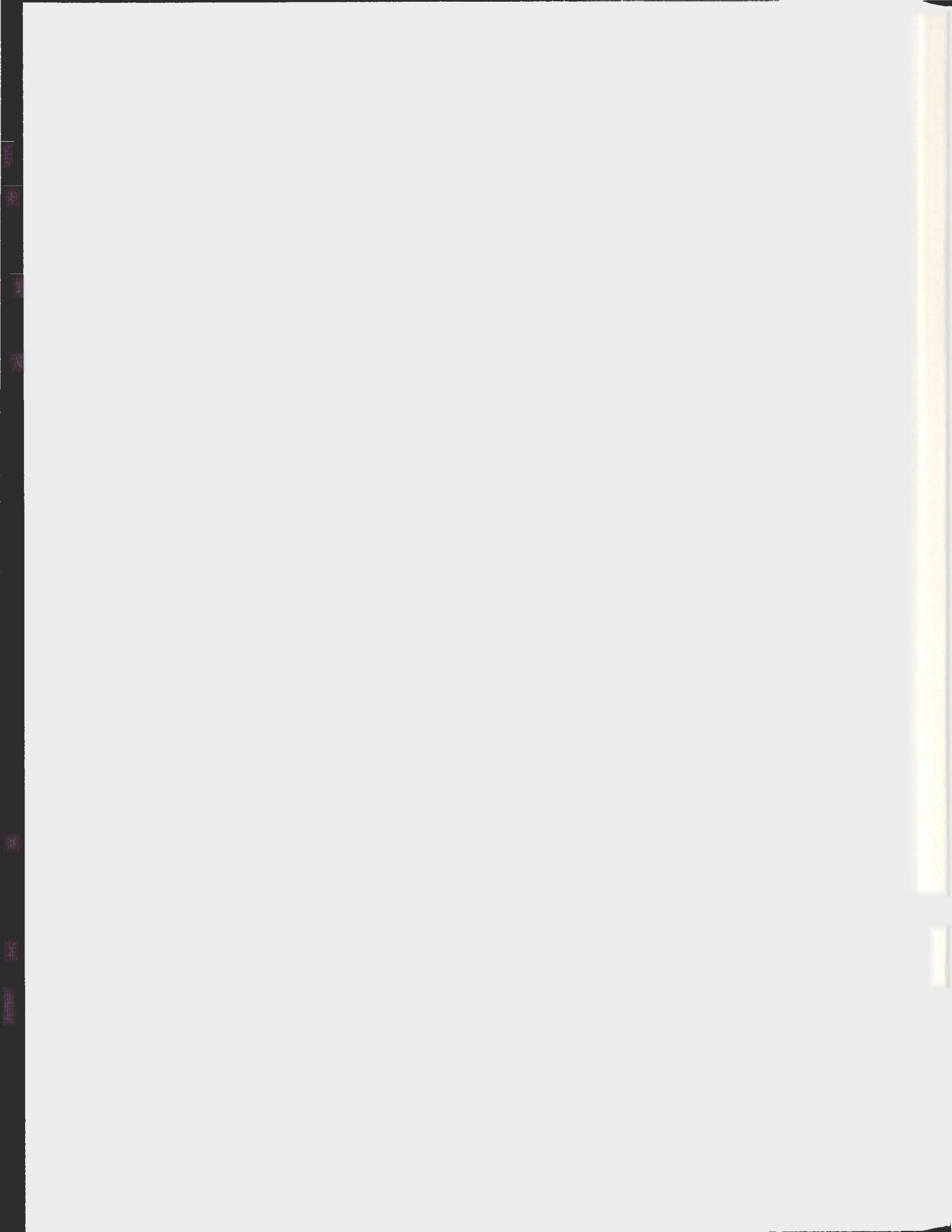


COLD ADAPTION OF ATLANTIC SALMON TROPOMYOSIN:
ROLE OF RESIDUE '77'

TOLULOPE OLUWASOMO IGE



**Cold Adaptation of Atlantic Salmon Tropomyosin: Role of
residue '77'**

Tolulope Oluwasomo Ige

**A Thesis Submitted to the School of Graduate Studies in
Partial Fulfillment of the Requirements for the Degree of
Master of Science**

**Department of Biochemistry
Memorial University of Newfoundland
St John's NL, Canada**

November 2012

Abstract

Tropomyosin from the fast skeletal (trunk) muscle of Atlantic salmon (*Salmo salar*) is an alpha-type isoform. It shares ~93% identity with a counterpart from rabbit skeletal muscle (20 amino acid substitutions out of a total of 284) but is less thermally stable.

An interesting aspect of the small heterogeneity is the replacement of lysine-77 in rabbit with threonine in salmon. In the case of the mammalian protein, the lysine in question is positioned to form ion pairs with aspartate-80 in the next turn of the same helix and also with glutamate 82 in the opposing helix of the coiled coil. Thus, at neutral pH, salmon tropomyosin loses two potential charge-charge (ion pair) interactions. The contribution of residue-77 to the properties of salmon tropomyosin has been investigated by mutating it to the amino acid in rabbit using site-directed mutagenesis, followed by circular dichroism, differential scanning calorimetry, affinity chromatography and limited proteolysis. A major finding of this research is that threonine in the 77th position of salmon tropomyosin is destabilizing compared to lysine in the same position. Reducing the number of ion pairs is concluded to be part of the structural means by which tropomyosin, and possibly other rod-shaped proteins, adapt to low temperature.

The specific details are outlined below in point form:

1. Atlantic salmon fast skeletal muscle alpha-tropomyosin cDNA was mutated to replace the threonine at position 77 with lysine using the QuickChange Lightning site directed mutagenesis kit. The mutation was confirmed by DNA sequencing.

2. Mutated and non mutated recombinant tropomyosins were obtained by expression in *E. coli* BL21 cells and chromatographically isolated.
3. The mutant salmon tropomyosin, containing Lys-77, exhibited a faster electrophoretic mobility than the non-mutant (Thr-77), in the presence of the detergent sodium dodecyl sulfate, which is attributable to a difference in detergent binding due to the extra charge. This electrophoretic shift was useful in the identification of amino-terminal peptides (see below, #7).
4. Far-UV circular dichroism was used to investigate the conformational stability of the recombinant salmon tropomyosins (ionic strength 0.1 M, +DTT, pH 7.0). The observed melting temperatures of the mutant (~45 °C) and non mutant (~40 °C) recombinant proteins differ by approximately 5 °C.
5. Differential scanning calorimetry was employed to monitor the thermal unfolding of non mutant and mutant recombinant tropomyosin (ionic strength 0.1 M, +DTT, pH 7.0) by direct heating. The observed melting temperatures of the mutant (~44 °C) and non mutant (~40.5 °C) protein differ by approximately 4 °C.
6. In an affinity chromatography experiment mutant tropomyosin bound more strongly to troponin-Sepharose 4B than the non mutant.

7. The time-course of limited chymotryptic or tryptic digestion (T, 25 °C) was monitored by SDS PAGE and found to be similar for mutant and non-mutant tropomyosins. Edman-based sequencing showed that the initial chymotryptic cleavage site in salmon recombinant tropomyosin (both mutant and non-mutant) is between Leu-11 and Lys-12. The second chymotryptic site is between Leu-169 and Val-170 which corresponds to the preferred site reported previously in rabbit alpha-tropomyosin.

Acknowledgements

First, I would like to express my sincere gratitude to my supervisor, Dr. David H. Heeley, for allowing me the opportunity to work in his lab and for his continuous guidance, encouragement and advice throughout this thesis.

I would also like to thank my supervisory committee members, Dr. M.E Mulligan and Dr. Valerie Booth, for their suggestions and guidance throughout this research project.

I would like to express my gratitude to the staff at CREATIT for their help and advice on DNA sequencing, also, to the technicians at the Advanced Protein Technology Center (Sick Children's Hospital, Toronto) for sequencing protein fragments.

I am grateful to Ms. Donna Jackman for her assistance and suggestions throughout the course of my research. I would like to thank Dr. Mike Hayley for his advice and Mr. Craig Skinner for his technical support throughout this research project.

I would like to express my gratitude to my former lab mate, Korie Fudge, for her help and suggestions throughout my research work.

I would like to acknowledge NSERC and the School of Graduate Studies at Memorial University of Newfoundland for providing funding for this research.

I am grateful to my husband, Adebayo, thanks for being there for me always. I would like to thank my parents, brothers, sisters and friends for all of their support regularly.

Finally, to God almighty, the maker of my destiny, thank you for seeing me through this stage of my life.

Contents

Abstract	II
Acknowledgements	V
Contents	VI
List of Figures	XI
List of Tables	XIII
Abbreviations	XIV

Chapter 1

Introduction

1.1	Structure of skeletal muscle	1
1.2	Tropomyosin	4
1.2.1	Tropomyosin isoforms	9
1.2.2	Naturally occurring modifications of tropomyosin	10
1.2.3	Association of tropomyosin with other proteins in the thin filament	11
	1.2.3.1 Tropomyosin-Actin association	11

1.2.3.2 Tropomyosin- Troponin association	14
1.3 Cold adaptation of tropomyosin	16
1.4 Fish tropomyosin	18
1.5 Mutation in tropomyosin sequence	21
1.6 Sites of proteolytic digestion in tropomyosin	21
1.7 Goals of study	22

Chapter 2

Materials and Methods

2.1 Reagents	24
2.2 Standard protocols	24
2.2.1 pH meter	24
2.2.2 Dialysis	24
2.2.3 Freeze drying	25
2.2.4 Determination of sample concentration	25
2.2.4.1 UV-Visible and Diode Array spectrophotometry	25

2.2.4.2	Nanodrop spectrophotometry	25
2.2.4.3	Bradford assay	26
2.2.5	Gel electrophoresis	26
2.3	Mutagenesis	27
2.3.1	Oligonucleotide primers	27
2.3.2	Purification of pTRC99A plasmid from E coli BL21 cells	27
2.3.3	Site directed mutagenesis	28
2.3.4	Transformation of E coli with XL10-Gold Ultracompetent Cells	29
2.3.5	Transformation of E coli with BL21 Cells	30
2.4	DNA Sequencing	30
2.5	Protein expression and isolation	32
2.6	Enrichment of Tropomyosin	33
2.6.1	Ion-Exchange Chromatography	33
2.6.2	Hydroxyapatite Chromatography	33
2.7	Affinity chromatography	34
2.8	Thermal stability studies	35
2.8.1	Circular dichroism	35
2.8.2	Differential scanning calorimetry	36
2.9	Proteolytic methods	36

2.9.1	Chymotrypsin and trypsin digestion	36
2.10	Electroblotting of digested samples	37
2.11	Data manipulation	37
2.11.1	cDNA sequences	37
2.11.2	Graphing	37

Chapter 3

Results and Discussion

3.1	Purification of DNA from BL21 Plasmids	38
3.2	Deoxyribonucleotide Sequencing	38
3.3	Expression of tropomyosin	40
3.4	Thermal stability studies	47
3.4.1	Circular dichroism	47
3.4.2	Differential scanning calorimetry	56
3.5	Affinity Chromatography	59
3.5.1	Effect of T77K mutation on the binding of tropomyosin to troponin	59
3.6	Proteolytic methods	64
3.6.1	Chymotrypsin and trypsin digestion	64

3.7	Sequencing of Proteolytic Fragments	68
-----	-------------------------------------	----

Chapter 4

General Discussion and Future Experiments

4.1	General Discussion	72
4.2	Future experiments	76
	References	78

List of Figures

Figure 1	Organization of skeletal muscle	2
Figure 2	Sequence of rabbit alpha-tropomyosin	7
Figure 3	Molecular ribbon diagram of a tropomyosin dimer	8
Figure 4	Major proteins of the thin filaments	12
Figure 5	Confirmation of the Thr77Lys tropomyosin mutation compared to the cDNA of Atlantic salmon fast muscle tropomyosin	39
Figure 6	SDS PAGE analysis of a lysate of IPTG-induced BL21 cells containing Thr77Lys tropomyosin	42
Figure 7	Q Sepharose Fast Flow chromatography profile of crude recombinant tropomyosin	44
Figure 8	Hydroxyapatite chromatography profile of recombinant tropomyosin	45
Figure 9	SDS PAGE analyses of highly-enriched mutant and non-mutant tropomyosins	46
Figure 10	Circular dichroism and thermally induced unfolding of the Thr77Lys mutant recombinant tropomyosin from Atlantic salmon	49
Figure 11	Normalized curve of the melting profiles of five samples of Thr77Lys	50
Figure 12	Thermally induced unfolding of the Thr77Lys mutant recombinant tropomyosin from Atlantic salmon as monitored by far-UV circular dichroism	51
Figure 13	Circular dichroism and thermally induced unfolding of	52

	the non-mutant recombinant tropomyosin from Atlantic salmon	
Figure 14	Normalized curve of the melting profiles of five samples of non-mutant recombinant tropomyosin	53
Figure 15	Thermally induced unfolding of the non-mutant recombinant tropomyosin from Atlantic salmon as monitored by far-UV circular dichroism	54
Figure 16	Comparison of the averaged, normalized melting curves of the mutant and the non mutant tropomyosin	55
Figure 17	Thermal denaturation of non mutant recombinant tropomyosin as monitored by differential scanning calorimetry	57
Figure 18	Thermal denaturation of mutant recombinant tropomyosin as monitored by differential scanning calorimetry	58
Figure 19	Affinity chromatography profile of non mutant recombinant tropomyosin	61
Figure 20	Affinity chromatography profile of mutant T77K recombinant tropomyosin	62
Figure 21	Comparison of the susceptibility of mutant T77K and non mutant tropomyosins to limited chymotryptic digestion at room temperature	66
Figure 22	Comparison of the susceptibility of mutant T77K and non mutant tropomyosins to limited tryptic digestion at room temperature	67

List of Tables

Table 1	Differences between the rabbit and salmon fast muscle tropomyosin	20
Table 2	Comparison of mutant and non-mutant tropomyosin	63
Table 3	Amino-terminal sequences of electroblotted fragments of recombinant Atlantic salmon tropomyosin	69

Abbreviations

ATP	Adenosine triphosphate
β -ME	β -mercaptoethanol
CAPS	N-cyclohexyl-3-aminopropanesulfonic acid
cDNA	Complementary deoxyribonucleic acid
dH ₂ O	Deionized water
DNA	Deoxyribonucleic acid
DTT	Dithiothreitol
EDTA	Ethylene diamine tetraacetic acid
EGTA	Ethylene glycol tetraacetic acid
ϵ_{280}	Extinction coefficient of protein at 280 nm
IPTG	Isopropyl β -D-1 thiogalactopyranoside
LB	Luria broth
MOPS	3-(N-morpholino) propanesulfonic acid
mRNA	Messenger ribonucleic acid
MWCO	Molecular weight cut off
NMR	Nuclear magnetic resonance
PCR	Polymerase chain reaction
pI	Isoelectric precipitation point
PMSF	phenylmethylsulfonyl fluoride
rpm	Revolutions per minute

RT	Room temperature
SDS	Sodium dodecyl sulfate
SDS PAGE	Sodium dodecyl sulfate polyacrylamide gel electrophoresis
TEMED	N, N, N', N' – tetramethylethylenediamine
TnC	Troponin C
TnI	Troponin I
TnT	Troponin T
Tris	Tris (hydroxymethyl) aminomethane
UV	Ultraviolet

Chapter 1

Introduction

1.1 Structure of skeletal muscle

Locomotion is an essential function for life in vertebrates; it is required for maintenance, reproduction and protection. This includes not only translocation but also the postural basis for stance and stability. The foundation for the buildup and regulation of force for locomotion is provided by skeletal muscle. Other types of muscle, such as smooth and cardiac, are involuntary muscles which are under control of the autonomic nervous system.

Skeletal muscle is made up of anatomically distinct units, which are attached to bones (via tendons) or other muscles (via ligaments) to support specialized movement. Individual muscles are composed of fascicles—assemblies of muscle fibers that are surrounded by a connective tissue sheath that can span the entire length of a muscle (Fig. 1A-C) (Lieber, 2002).

Each fiber (diameter between 10 and 100 μ m) is one single cell, which is usually multinucleated, whose cytosol is confined by a single membrane called the sarcolemma. The sarcolemma protrudes into the muscle fiber at regular intervals forming transverse tubules (t-tubules). T-tubules provide an important pathway for electrical signals from the surface to the core of the cell, where they lie adjacent to the cisterns of the sarcoplasmic reticulum (SR), the intracellular calcium ion store of muscle cells (King *et al.*, 2004).

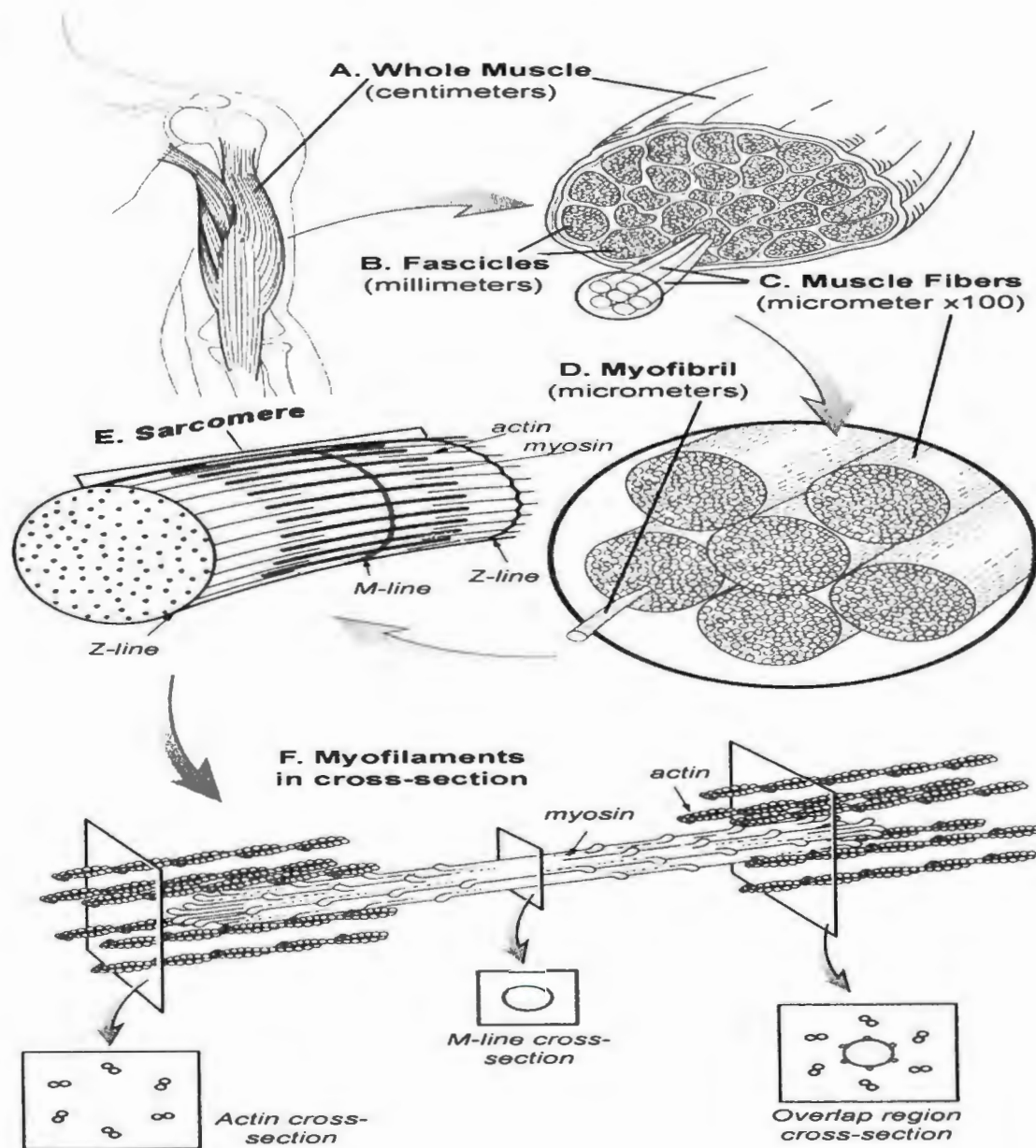


Figure 1: Organization of skeletal muscle. Whole skeletal muscles are composed of numerous fascicles of muscle fibers. Muscle fibers are composed of myofibrils arranged in parallel. Myofibrils are composed of sarcomeres arranged in series. (from King A.M., Loiselle D.S., and Kohl P. (2004) Force generation for locomotion of vertebrates: Skeletal muscle overview. *IEEE J. Ocean. Eng.* 29(3): 684-691. Used with permission (© 2004 IEEE).

Fibers contain densely packed regular bundles of myofibrils, the contractile units of muscle. Myofibrils are made up of thick (myosin) and thin (actin, tropomyosin and troponin) protein filaments. Muscle also contains a host of other proteins which are required for various aspects of filament structure, including anchoring (e.g. α -actinin), end ‘capping’ (e.g. tropomodulin (Yamashiro *et al.*, 2010) and Cap Z) and spatial organization (e.g. titin (Wang *et al.*, 1979) and nebulin) as well as enzymes for the production of adenosine tri-phosphate and creatine phosphate. These filaments are arranged in a hexagonal pattern and interdigitate (Fig. 1F). Myofibrils are organized in highly structured sarcomeres (Fig. 1E) (King *et al.*, 2004).

The regular packing of myofibrils in the sarcomere gives rise to the typical cross striation of skeletal muscle where the region of the sarcomere that contains the (thick) myosin filaments is optically more dense (anisotropic: A-band) than the remainder of the sarcomere that contains only the (thin) actin filaments (isotropic: I-band). The center of the I-band is marked by a narrow dark line, referred to as the Z-line. The distance between two Z-lines is the sarcomere length. Z-lines provide the anchor point for actin filaments, which extend on both sides of each Z-line. It is important to note that, functionally, sarcomeres consist of two half-sarcomeres whose force generators have opposite polarity.

Myosin filaments ($\sim 1.6 \mu\text{m}$ in length) consist of several hundred myosin molecules that are each around $0.15 \mu\text{m}$ long (Alexander, 2003). The center part of the filament is smooth (no myosin heads) and interlinked with neighboring myosin filaments of the same sarcomere at the M-line (Fig. 1F) Within a sarcomere, myosin molecules are assembled “in register” by virtue of titin—a

gigantic molecule that tethers each half of a myosin molecule to its adjacent Z-line (Gregorio *et al.*, 1999). Myofibrils also contain mitochondria known as the “power station” of the cell, often arranged in parallel with individual sarcomeres (King *et al.*, 2004).

Myofibrils are comprised of overlapping thick and thin filaments, which slide past each other to produce muscle contraction (Huxley, 1974). The thick filament is composed primarily of myosin, which contains the ATPase activity of the myofibril and forms cross-bridges with actin. About 400 myosin molecules assemble to form a filament, which interacts with actin filaments containing about the same number of actin monomers (Hanson and Lowy, 1963; Huxley, 1963). Myosin therefore has multiple functions which include filament formation, ATPase activity, and reversible combination with actin. The use of proteolytic enzymes helped reveal which regions of the myosin molecule were responsible for each of these different functions (Gergely, 1950; Perry, 1951).

1.2 Tropomyosin

Tropomyosin was discovered by Bailey (1946). It is found in striated (skeletal and cardiac) muscle, smooth muscle and (at lower quantities) in non-muscle tissues (Smillie, 1979). The properties of tropomyosin have been unveiled in detail through biochemical and biophysical studies (Perry, 2001). Studies carried out in solution have shown that tropomyosin, in combination with troponin (a triple subunit complex), serves as an allosteric regulator of striated muscle activity (Gordon *et al.*, 2000). At the same time, tropomyosin has been proposed to shift in its physical position on actin. Such movement is central to the Steric Blocking hypothesis

(Huxley, 1969 and 1972). The hypothesis, originally based on observations from X-ray diffraction, has undergone revision over the years and in recent times the use of three-dimensional imaging of thin filament electron micrographs has provided a way of testing it. Analysis of thin filaments prepared under activating (high calcium, presence of rigor) or relaxing (low calcium, absence of rigor) conditions documents a shift in tropomyosin such that myosin binding sites are either uncovered or covered.

Tropomyosin is highly α -helical (Cohen and Szent-Gyorgyi, 1957) and yields a characteristic circular dichroism spectrum with strong minima at 208 and 222nm. Sedimentation (Woods, 1967) and sequencing studies (Hodges and Smillie, 1972) indicated that the native structure is that of a double stranded coiled coil (Figure 3). The production of a disulfide linkage between the two chains (Johnson and Smillie, 1975, Lehrer 1975) confirmed this view and also demonstrated that the chains are parallel to each other (i.e. the N-termini occur at the same end of the dimer) and non-staggered.

The sarcomeric forms of tropomyosin contain 284 amino acids per chain (Stone and Smillie, 1978) yielding a molecular weight of 66,000 Dalton (Woods, 1967). An outstanding feature of the primary structure is the presence of non-polar residues at the first (residue 'a') and fourth (residue 'd') of a heptapeptide unit (where the seven residues are *a,b,c,d,e,f,g*). These so-named 'core' residues create a hydrophobic stripe along the long axis of the helix which promotes chain-chain association. Since the seam winds around this axis, the two chains have to coil in order to maintain contact. Such an arrangement had been predicted by Crick (1953). Crick's "knobs" and "holes" hypothesis envisaged that at the interface of the coiled-coil a side-chain in

one helix would pack into a space in the other. Subsequent research has confirmed that the stability of the coiled coil is produced mainly by these hydrophobic interactions (Greenfield and Hitchcock-Degregori, 1995). Additional stability is provided by ionic interactions between charged residues in the *e* and *g* positions (Williams and Swenson, 1981) as indicated in Figure 2B.

Another feature of muscle tropomyosin is its ability to self-polymerise end-to-end. The nature of this interaction, which allows tropomyosin to form a continuous strand along the actin filament, was revealed by electron microscopy and low-angle X-ray diffraction of tropomyosin paracrystals (Cohen and Longley, 1966) to entail an overlap of two connecting (and elongated) dimers. The number of residues involved in the interaction was later investigated by removal of residues from either end of tropomyosin (Ueno *et al.*, 1976; Mak and Smillie, 1981; Dabrowska *et al.*, 1983; Goonasekara *et al.*, 2007). Ultimately, NMR showed a merger of the first and last eleven amino acids (Greenfield *et al.*, 2006). Electrostatic interactions are thought to play a role in overlap formation since these regions have opposing net charges at neutral pH. Presently, however, there is not a unified model as to the exact structural details of the overlap. Perhaps the dominant view entails the N-termini ‘dovetailing’ with an opening of the C-termini (Greenfield *et al.*, 2006 and Frye *et al.*, 2010).

The task of structural determination at high resolution has been hampered by the very high water content of tropomyosin crystals. The best resolution achieved for the whole molecule is 7 Angstroms (Whitby and Phillips, 2000) (Figure 3). However, atomic-level resolution has been obtained by crystallising sections of tropomyosin, specifically residues 1-80 (Brown *et al.*, 2001)

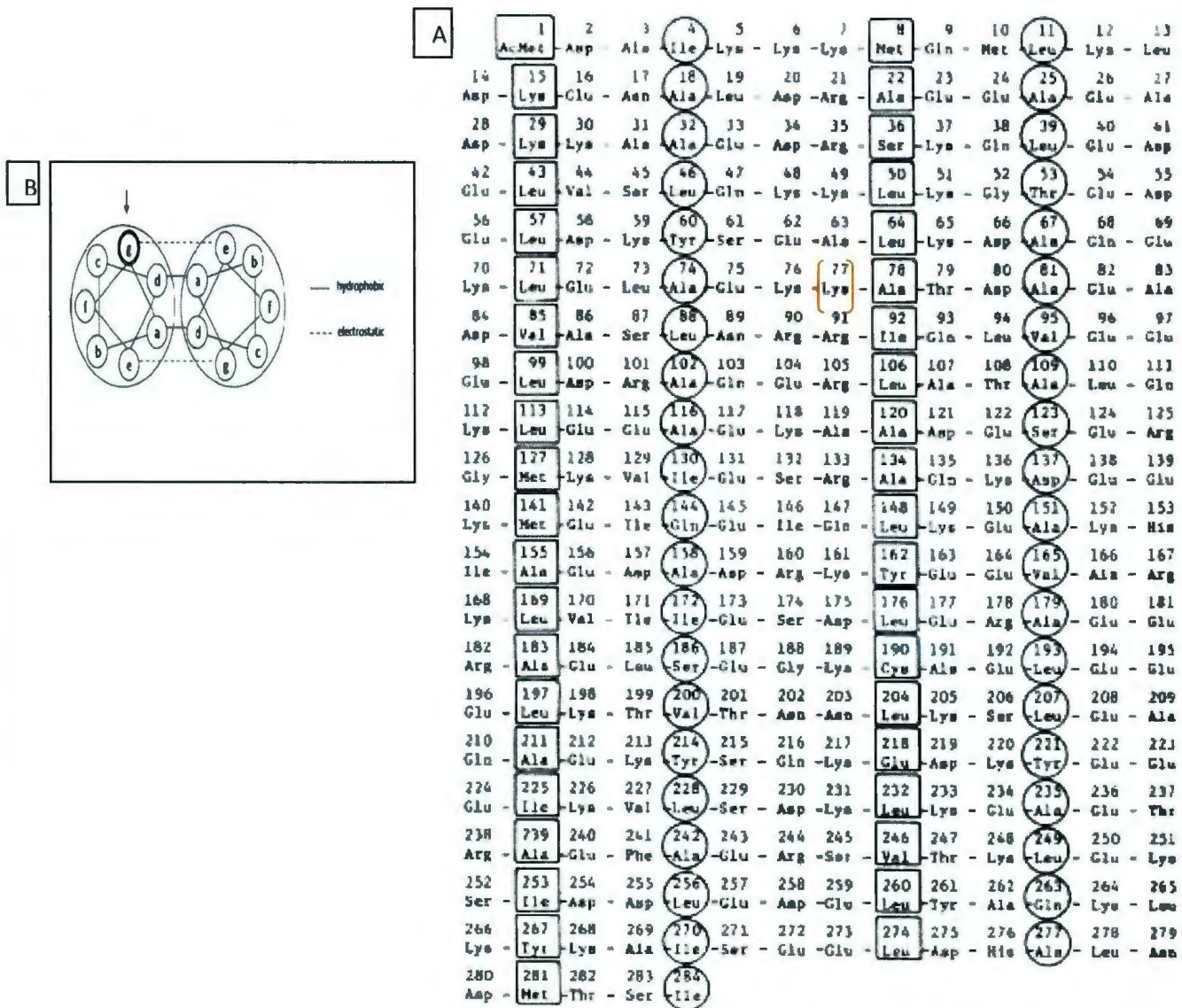


Figure 2: (A) Sequence of rabbit alpha-tropomyosin (after Hodges et al 1972). Core positions are indicated by boxes and circles. Orange bracket shows the position of the mutation of interest. (B) Heptad positions in coiled coil cross section (after Smillie 1979). Arrow indicates location of the mutation in the heptapeptide repeat and along the seven pseudorepeats of tropomyosin. Residues 'a' and 'd' are typically hydrophobic and maintain coiled-coil structure. Residues 'g' and 'e' are typically charged amino acids that additionally stabilize the protein through ionic interactions.

and 89-208 (Brown *et al.*, 2005). One of the insights provided by these structures concerns clusters of core alanines. These clusters are thought to destabilise tropomyosin (relative to larger non-polar side chains such as leucine) and thereby build flexibility into the molecule enabling it, for example, to wrap itself around an actin filament.

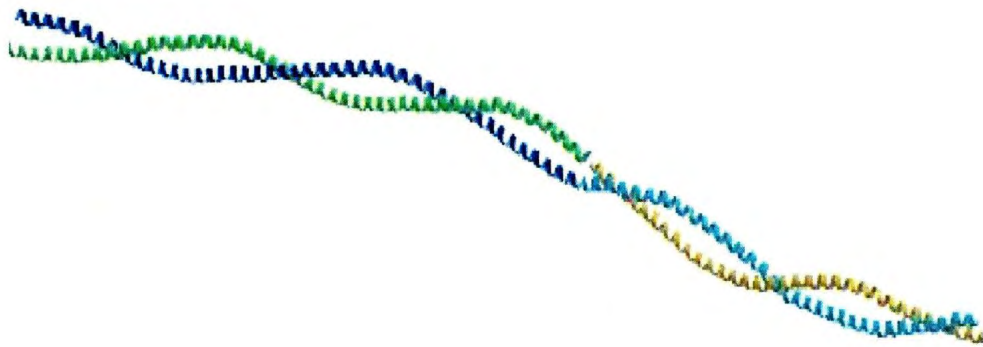


Figure 3: Molecular ribbon diagram of a tropomyosin dimer

Image from the RCSB PDB (www.pdb.org) of PDB ID: 1C1G

Whitby F.G., Phillips Jr. G.N. (2000) Crystal structure of tropomyosin at 7 Angstroms resolution.

Proteins 38: 49-59

1.2.1 Tropomyosin Isoforms

Distinct isoforms of tropomyosins are present in muscle (skeletal, cardiac and smooth), and various non-muscle cells. The first evidence that there are multiple forms of tropomyosin came from electrophoresis separations performed in the presence of SDS (Cummins and Perry, 1973). Two variants were observed, called α and β . The basis of the separation is not due to a true difference in mass but net charge which affects the interaction with SDS. β -tropomyosin is predicted to have a higher net negative charge at neutral pH than α due to substitution at two positions (Ser229Glu and His276Asn) (Mak *et al.*, 1980). Mammalian skeletal muscles contain both forms of tropomyosin but the molar ratio varies depending on the muscle (Heeley *et al.*, 1985) and the stage of development (Amphlett *et al.*, 1976).

The various isoforms arise from the combination of multiple genes, alternative splicing and multiple promoters. Four different tropomyosin genes have been characterized in the vertebrates, although it is not certain that all species contain the full complement. Each of the genes has been named after the proteins they encode. For example, α and β genes are named after striated muscle α and β -tropomyosins, respectively. The TM-4 and TMnm genes are named after the rat fibroblast TM-4 and human fibroblast TM30 nm isoforms, respectively (Lees-Miller and Helfman, 1991). In the Human Genome Project, tropomyosin genes are referred to as TPM 1, 2, 3 and 4.

1.2.2 Naturally occurring modifications of tropomyosin

Acetylation of the amino-terminal α -amine of proteins is a widespread modification in eukaryotes. The reaction is catalyzed by amino-terminal acetyltransferases, which occurs predominantly during protein synthesis and appears to be irreversible. Acetylation of tropomyosin affects coiled-coil stability (Greenfield *et al.*, 1994), and is especially important for overlap formation (McLachlan and Stewart, 1975). Bacterially-expressed (unacetylated) tropomyosin polymerises poorly and binds weakly to F-actin (Hitchcock-DeGregori and Heald 1987) whereas tropomyosin expressed in an insect cell has similar properties to muscle tropomyosin (Urbancikova and Hitchcock-DeGregori 1994).

Phosphorylation can occur on amino acid Ser 283 of striated muscle tropomyosins (Mak *et al.*, 1978) but this residue is not conserved in all isoforms such as those in smooth muscle (Sanders and Smillie 1985). Covalently bound phosphate was first detected in tropomyosin from the skeletal muscle of a frog that had been injected with ^{32}P -orthophosphate (Ribulow and Barany, 1977). Subsequently, this modification has been found in the striated muscle tropomyosins of rabbit, chicken, fish, rat and mouse (Montarras *et al.*, 1981; Heeley *et al.*, 1982; Heeley and Hong, 1994). Studies have shown that phosphorylation increases head-to-tail polymerization as well as the steady-state rate of hydrolysis of regulated actomyosin MgATPase (Heeley *et al.*, 1989 and Heeley, 1994). Later research using phosphorylated and unphosphorylated shark tropomyosin confirmed the earlier results (Hayley *et al.*, 2008).

1.2.3 Association of tropomyosin with other proteins in the thin filament

The skeletal-muscle thin filament (Figure 4) is composed of actin, tropomyosin, and troponin in a 7: 1: 1 molar ratio (Potter, 1974, Yates and Greaser, 1983). Each of these thin-filament proteins has specific interactions with the other thin-filament proteins, which allow self-assembly of actin, tropomyosin, and troponin reconstituted after purification (Zot and Potter, 1987).

1.2.3.1 Tropomyosin-Actin association

Actin was discovered by Straub (1942). At low ionic strength, actin molecules are stable as monomers (G-actin). Upon addition of salt, especially divalent cations, actin polymerizes into huge filaments. The high asymmetry of the polymerized actin (F-actin) is indicated by its high viscosity and strong double refraction of flow (Straub, 1942). Actin filaments are polar entities as dramatically shown by decoration with rigor myosin heads (Huxley, 1963). The barbed and pointed ends respectively correspond to the ends of slower and faster extension (Woodrum *et al.*, 1975). Sarcomeric F-actin does not change in length because, as mentioned in the Introduction, the two ends are capped.

Muscle actin contains 375 amino acids (Collins and Elzinga, 1975). The first atomic structure of G-actin was obtained in complexation with DNase I (Kabsch *et al.*, 1990). Later, the structure of chemically modified G-actin was solved in the absence of an actin binding protein (Otterbein *et al.*, 2001). Although an atomic structure for F-actin is unavailable a model has been constructed using the structure of the monomer (Holmes *et al.*, 1990).

A

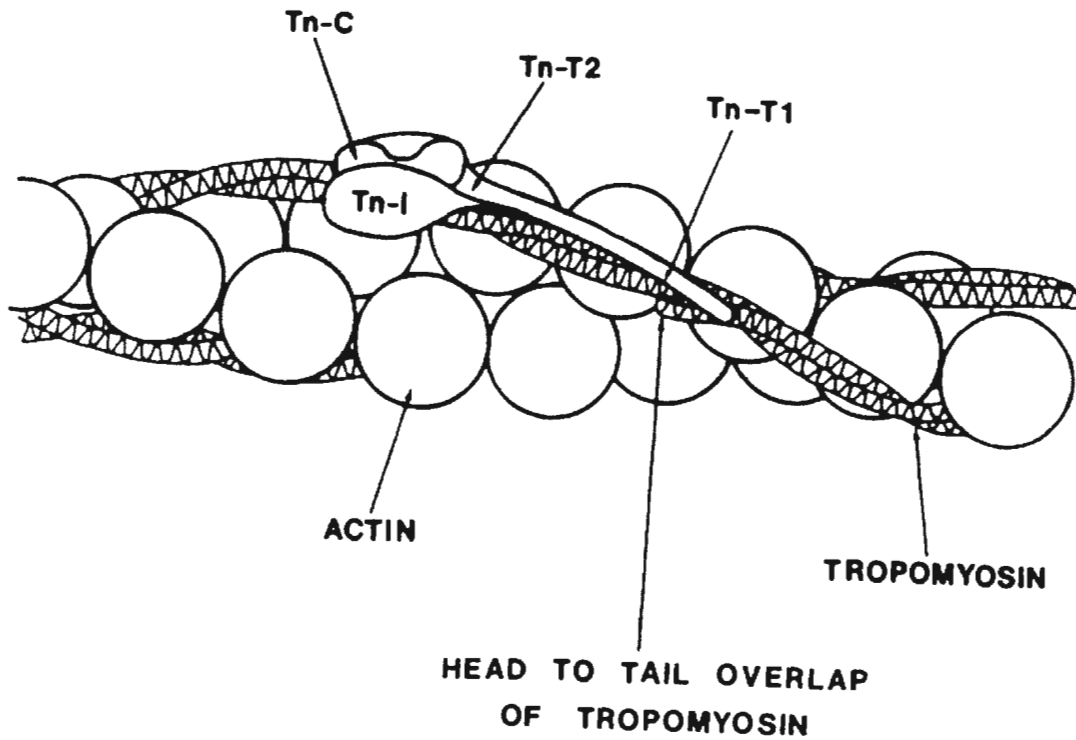


Figure 4: Major proteins of the thin filaments

Heeley *et al.*, 1987. *J. Biol. Chem.* 262, 9971-9978 (Drawing provided by D.H Heeley)

Key, Tn-C (troponin C); Tn-I (troponin I); Tn-T2 (carboxy-terminal chymotryptic fragment of troponin T) and Tn-T1 (amino-terminal chymotryptic fragment of troponin T).

The sequence of tropomyosin can be divided into actin binding segments (or periods) of approximately 40 amino acids. As stated earlier, one molecule of muscle tropomyosin (of 284 amino acids) spans seven actin monomers (Figure 4). The shorter forms of tropomyosin from non-muscle and yeast span six or five. Detailed sequence analysis of tropomyosin revealed two sets of 7 quasi-equivalent repeating regions of acidic and nonpolar residues throughout the length of each chain that could serve as actin-binding sites (Parry, 1974; Stewart and McLachlan, 1975; Stone *et al.*, 1974). Stewart & McLachlan (1975) showed that there are 28 acidic zones in the tropomyosin dimer which are exposed on the surface of the molecule and arranged in 14 opposing pairs such that four sets of seven zones occur at 90° to each other. These acidic zones may interact with acidic regions on actin through Mg²⁺ bridges or with positive regions on actin via salt bridges; hydrophobic interactions between nonpolar groups may provide additional stability (Stewart & McLachlan, 1975). Phillips *et al.* (1980) have suggested, based upon the apparent dynamic nature of tropomyosin in crystals, that interactions between tropomyosin and actin are not so strictly limited. This led to the proposition that tropomyosin is continually changing connections with actin, producing a net effect of relaxation or contraction.

An important step in investigating the interaction between actin and tropomyosin was the use of recombinant nucleic acid technology to create deletions of varying length in the second actin binding period, residues 47–88 (Hitchcock-DeGregori and Varnell, 1990). Reconstituted thin filaments containing a non-fusion tropomyosin with half of, or the entire, period 2 missing displayed good regulatory function. However, this was not true of tropomyosin in which two-thirds of period 2 had been removed (Hitchcock-DeGregori and Varnell, 1990). These findings show that there is a periodicity within the tropomyosin sequence that governs actin binding.

More recent research (reviewed in Hitchcock-DeGregori and Singh, 2010) has demonstrated that the seven actin binding periods are not equivalent. Alteration of periods 1 and 5 strongly perturbs actin affinity whereas the other five are less sensitive to manipulation in this regard.

The ability of tropomyosin to self-polymerize greatly strengthens actin binding (Wegner, 1979). Removal of either the first or last 9-11 residues of striated muscle α -tropomyosin results in a large reduction in actin affinity (Ueno *et al.*, 1976; Mak and Smillie, 1981; Dabrowska *et al.*, 1983; Goonasekara *et al.*, 2007). Since troponin interacts with tropomyosin in the region of Cys190 (see below) it is possible that Ca^{2+} -dependent changes in this area could affect tropomyosin-actin binding through an effect on the overlap region of tropomyosin. Although this binding change could be mediated by conformational changes in tropomyosin, it now seems likely, based upon the above findings, that the change would additionally or alternatively be mediated by conformational changes in actin (Butters *et al.*, 1993).

1.2.3.2 Tropomyosin- Troponin association

Troponin was discovered by Ebashi and Kodama (1965). The molecular masses of the three troponin subunits were first determined from the amino acid sequences of the proteins obtained from rabbit skeletal muscle: troponin C (TnC, Mr = 18,000 Da) (Collins *et al.*, 1977), troponin T (TnT, Mr = 30,500 Da) (Pearlstone *et al.*, 1977a) and troponin I (TnI, Mr = 21,000 Da) (Wilkinson and Grand, 1975). TnC is the calcium binding subunit, TnT binds to tropomyosin and TnI is the inhibitory subunit (Greaser and Gergely, 1971, 1973).

The calcium-regulated control of striated muscle contraction involves the interaction of troponin with tropomyosin on the muscle filament (Pearlstone and Smillie, 1982). Studies have demonstrated that the two regions of TnT are involved in interactions with tropomyosin (Mak and Smillie, 1981). One of these, represented by the soluble cyanogen bromide fragments CB1 (residues 1-151) and CB2 (residues 71-151) and the chymotryptic fragment T1 (1-158), is bound close to or at the carboxy-terminal end of tropomyosin. The second region, represented by the chymotryptic fragment T2, is believed to bind close to cysteine-190 of tropomyosin (Cohen *et al.*, 1972; Phillips *et al.*, 1980; Stewart and McLachlan, 1975; Pato *et al.*, 1981; Morris and Lehrer, 1984). The CB2 subfragment (residues 71-151) interacted with tropomyosin, but less effectively than CB1 (Jackson *et al.*, 1975). Subfragment CB3 (residues 1-70) did not bind to tropomyosin (Jackson *et al.*, 1975; Pearlstone and Smillie, 1977). However, Nuclear Magnetic Resonance (¹H-NMR) study carried out at high concentrations of proteins indicated that CB3 does contribute significantly to the specificity of the interaction between CB1 and tropomyosin, and that the interaction of CB2 with tropomyosin is nonspecific (Brisson *et al.*, 1986).

Ohtsuki (1979) demonstrated that TnT is elongated and spans about 130 Å along tropomyosin, and that TnC and TnI bind together at one end of TnT. Circular dichroism data by Pearlstone and Smillie (1978) show a high helical content in residues 71 - 151 of TnT; residues 159-227 contain a strong heptapeptide repeat similar to that in the tropomyosin sequence (Parry, 1981). Thus these two peptides of TnT may interact with tropomyosin in a coiled coil or triple-stranded coiled coil (Mak *et al.*, 1983). The interaction of troponin with tropomyosin may stabilize the overlap region and/or have a role in the transduction of the Ca²⁺-binding signal for muscle activation (Phillips *et al.*, 1980, Flicker *et al.*, 1982).

The atomic structure of TnC was reported in 1985 (Herzberg and James, 1985) but the whole troponin complex proved more difficult to crystallise. Two atomic structures are available for the globular core of troponin (TnI+TnC+carboxy-terminal one-third of TnT) in both Ca²⁺ - bound and free forms (Takeda *et al.*, 2003; Vinogradova *et al.*, 2005). Missing from these structures is the elongated tail of TnT which comprises the amino-terminal two-thirds of the molecule. The globular core contains two important structural elements: (i) the “IT” arm which is made up of the high affinity metal ion sites of TnC and the aforementioned coiled-coil between subunits I and T and (ii) the regulatory head consisting of the ‘trigger’ calcium sites of TnC and the TnI inhibitory peptide (Syska *et al.*, 1976, Talbot and Hodges, 1981). These structures demonstrated that the orientation of the inhibitory peptide is calcium-sensitive.

1.3 Cold-adaptation of tropomyosin

Despite the fact that a much greater proportion of the earth’s environment is cold rather than hot, much less is known about psychrophilic, cold-adapted organisms compared with mesophiles or thermophiles living at high temperatures. Psychrophiles are extremophilic organisms that are capable of growth and reproduction in cold temperatures below 15 °C. Mesophiles grow best in moderate temperature, neither too hot nor too cold, typically between 20 and 45 °C.

Thermophiles thrive at relatively high temperatures greater than 50 °C (Gerday *et al.*, 1997; Greaves and Warwicker, 2007).

Recent accumulation of structural data on psychrophilic proteins is beginning to shed light on their functional and structural characteristics (e.g. Feller and Gerday, 1997). Most of the research that has been carried out on proteins from psychrophilic organisms is on globular proteins. Gianese *et al.* (2001) described the general features of structural adaptation of proteins to low temperatures. Their results indicated that charged residues (e.g. Glu, Arg and Lys) tend to be replaced in psychrophilic proteins at exposed sites within α -helices or coil regions and that this replacement is one of the mechanisms of low-temperature adaptation shared by most of the cold-adapted proteins. It has been suggested by several other authors (e.g. Greaves and Warwicker, 2009; Xiao and Honig, 1999) that ion pairs, hydrogen bonds and electrostatic interactions in which charged residues are involved play an important role in protein stabilization, particularly at high temperature. In view of this, psychrophiles have increased loop sizes and decreased numbers of ion pairs, hydrogen bonds and hydrophobic contacts (Greaves and Warwicker, 2009; Greaves and Warwicker, 2007; Gianese *et al.*, 2002) compared to mesophiles and thermophiles. These differences provide psychrophilic proteins with the necessary flexibility to function at low temperature. They also account for the fact that such proteins are generally unstable at mesophilic temperatures and higher.

Some research has been done on the stability of the non-globular protein tropomyosin which confirms that the core position amino acids ("a" and "d") are critical to its stability. Hayley *et al.* (2008) reported that shark tropomyosin has three core amino acid substitutions compared to rabbit tropomyosin (Stone and Smillie, 1978). In each case, the equivalent amino acid is replaced by a hydroxyl-containing one (e.g. Thr179Ala, Ser190Cys and Ser211Ala). Examination of shark and rabbit tropomyosin indicates that the shark isoform has a reduced conformational

stability through most of its structure compared to the rabbit isoform which is a result of the core amino acid substitutions (Hayley *et al.*, 2011).

1.4 Fish Tropomyosin

Fish have been under utilized as a source of muscle tissue and muscle protein for biochemical studies. However, the musculature of fish offers a number of advantages to the research of muscle contraction. Bony (teleost) fish contain a simple and long range, structural order of myofilament lattices which is well suited for X-ray diffraction studies (Harford and Squire, 1990). Further, while most mammalian muscles are composed of an intermingled mixture of fast and slow fibres, these cell types are anatomically separated in the swimming muscles in the trunk, thereby facilitating the dissection of muscle for the isolation of fibre-specific protein isoforms (Heeley and Hong, 1994). In the majority of round-bodied fish, the slow-contracting (darker) muscle is confined to a seam along the lateral line, running from the back of the head to the caudal fin. This muscle is needed for constant low-speed swimming (Johnston *et al.*, 1975; Johnston, 1980; Bone and Marshall, 1982). The fast-contracting (lighter) muscle (>90% of total myotome, in most species) represents an 'emergency power pack' (Bone and Marshall, 1982) for the purposes of predation or escape.

The skeletal (fast and slow) and cardiac muscles of Atlantic salmon (*Salmo salar*) have been shown to comprise a simple pattern of tropomyosin isoforms (Heeley and Hong, 1994; Jackman *et al.*, 1996). Fast and cardiac muscle contain one unique variant. Slow muscle contains two (in unequal proportions). The fast muscle type of Atlantic salmon tropomyosin was used for this

study. Based on its cDNA sequence (accession number NP_001117128, Heeley *et al.*, 1995) it is an alpha-type isoform which contains 20 amino acid substitutions compared to the rabbit counterpart (accession number NM_001105688) (Stone and Smillie, 1978). However, despite the small number of replacements, NP_001117128 varies significantly from the mammalian version in terms of its conformational stability (Heeley *et al.*, 1995). Both halves of the salmon protein were found to be of comparatively lower stability (Goonasekara and Heeley, 2008).

The sequence of Atlantic salmon fast skeletal tropomyosin, containing 284 amino acid residues, is shown below in single-letter code:

```
mdaiKKkmqm lkldkenald raegaegdKk aedkskqlE ddIvalqkkl kgtedeldky  
seslkdaqek levaektatd aadvaslnr riqlveeeld raqerlatal tkleeaekaa  
desergmkvi enraskdeek melqdiqlke akhiaeeadr kyeevarklv iiesdlerte  
eraelsegkc seleeelktv tnnlksleaq aekysqkedk yeeeikvltd klkeetrae  
faersvakle ktiddledel yaqklkykai seeldnalnd mtsi
```

Of the 20 substitutions alluded to above (Table 1), only one affects a core amino acid specifically, residue-179 which is a threonine in salmon and an alanine in rabbit (this residue was recently studied in this laboratory). Of interest in the present study is residue-77 which is a threonine in salmon and a lysine in its rabbit counterpart. Given the ionic interactions which can occur in tropomyosin (Figure 2) this particular substitution was viewed as one of the potentially important determinants of the unique properties of salmon tropomyosin and was selected for investigation.

Table 1: Differences between the rabbit and salmon fast muscle tropomyosin

Position	Heptapeptide designation	Salmon	Rabbit
24	c	Gly	Gln
27	f	Gly	Ala
35	g	Lys	Arg
42	g	Asp	Glu
45	c	Ala	Ser
63	g	Ser	Ala
73	c	Val	Leu
77	g	Thr	Lys
111	f	Thr	Gln
132	f	Asn	Ser
135	b	Ser	Gln
143	c	Leu	Ile
145	e	Asp	Glu
157	c	Glu	Asp
179	d	Thr	Ala
191	b	Ser	Ala
229	e	Thr	Ser
247	b	Ala	Thr
252	g	Thr	Ser
276	c	Asn	His

1.5 Mutation in tropomyosin sequence

The pattern of charged residues in the "e" and "g" positions favours interhelical ion pair formation. The amino acid in position "77" ('g') is threonine in salmon and lysine in its rabbit counterpart. In the case of the mammalian protein, the lysine is positioned to form ion pairs with aspartate-80 in the next turn of the same helix and also glutamate-82 in the opposing helix of the coiled coil. Thus, at neutrality, salmon tropomyosin loses two charge-charge interactions. By inference, adjusting the number of ion pairs is one way in which to retain flexibility of tropomyosin at low temperature. The mutant Thr77Lys was made to examine the individual and additive effect of that residue on the conformational stability.

The threonine residue was mutated to a lysine because lysine is the residue that is present at the same position in rabbit skeletal tropomyosin (Stone and Smillie, 1978).

1.6 Sites of proteolytic digestion in tropomyosin

In this present study, chymotrypsin and trypsin were used to study the digestion patterns of mutant recombinant tropomyosin and non-mutant recombinant tropomyosin. Pato *et al.* (1981a) examined the digestion patterns of rabbit striated α -tropomyosin by limited trypsin and chymotrypsin proteolysis. They showed chymotrypsin initially cleaved tropomyosin on the carboxy-terminal side of Leu-169. This residue is in the core of the protein and was believed to be fairly inaccessible to the enzyme. The researchers proposed that this residue is in a destabilized area due to the presence of several bulky hydrophobic residues at positions 169-172

(-Leu-Val-Ile-Ile-). They also speculated that an aspartic acid (Asp175) in a 'g' position results in an electrostatic repulsion with Glu180 which contributes to that region's instability.

1.7 Goals of study

The main goal of this study was to characterize the influence which a particular amino acid in salmon fast muscle tropomyosin has on the protein's stability. The residue of interest was threonine77. It was hypothesized that the threonine77 increases flexibility because it is a hydrophilic amino acid located in the electrostatic region of the protein.

In this present study, the contribution of residue-77 to the properties of salmon tropomyosin has been investigated using site-directed mutagenesis, limited proteolysis in conjunction with Edman-based sequencing, affinity chromatography, differential scanning calorimetry and circular dichroism. The findings described herein offer insight into the factors which modulate conformational stability of rod-shaped proteins in psychrophiles, which have not been studied to the same extent as globular proteins.

The specific aims are:

1. Create a Thr77Lys mutant of salmon fast skeletal tropomyosin using site directed mutagenesis
2. Isolate enriched protein samples using salt-precipitation and ion-exchange and hydroxyapatite chromatography

3. Use a circular dichroism spectrophotometer and differential scanning calorimeter to monitor and compare the heat-induced unfolding of the mutant and the non-mutant recombinant tropomyosins in order to determine their melting temperatures
4. Use chymotrypsin and trypsin digestion to compare the cleavage patterns of the non-mutant and mutant tropomyosin
5. Determine initial proteolytic cleavage sites by Edman-based sequencing
6. Determine the binding affinity of the tropomyosins to troponin using affinity chromatography

Most of the results of this thesis were presented in preliminary form at the 56th Annual Biophysical Society Meeting in San Diego: Ige, T.O, Fudge, K.R. and Heeley, D.H (2012) Mutagenesis of a tropomyosin isoform from Atlantic salmon.

Chapter 2

Materials and methods

2.1 Reagents

Unless otherwise stated, all reagents were obtained from Sigma-Aldrich (Oakville, ON) or Fisher Scientific (Mississauga, ON). All chromatography columns and media were obtained from GE Healthcare (Uppsala, Sweden). Custom-made oligonucleotide primers were obtained from Operon (Huntsville, Alabama).

2.2 Standard protocols

2.2.1 pH meter

A refillable combination calomel glass electrode (FuturaTM, 12×130 mm, Beckman) attached to a Beckman Φ 32 pH meter was used for all pH measurements. The electrode was calibrated daily using standard solutions of pH 4.00 and pH 7.00.

2.2.2 Dialysis

Dialysis was performed using 10 mm or 45 mm width; 12,000- 14,000 MWCO (Molecular Weight Cut Off) dialysis tubing (Spectrum, California). Dialysis tubing was prepared by heating in 2 L of approximately 10 mM Sodium bicarbonate, 1 mM EDTA to 70⁰C. This was followed by extensive washing (3-4 changes) with deionised water. The tubing was left to soak overnight in deionised water and then stored in 70% (v/v) ethanol at 4 °C. Prior to use, the dialysis tubing was washed thoroughly with deionised water.

2.2.3 Freeze Drying

Dialysed samples were frozen with liquid nitrogen and freeze dried on a FreeZone^(R) CFC-Free Freeze Dry System (LABCONCO). The freeze-dried samples were then stored in the fridge until further analysis.

2.2.4 Determination of sample concentration

2.2.4.1 UV-Visible and Diode Array spectrophotometry

Protein concentrations were determined by UV absorbance measurements in either a Beckman DU-64 spectrophotometer or an Agilent 8453 Diode Array spectrophotometer. Freeze-dried tropomyosin samples were dialysed using narrow dialysis tubing (10 mm) overnight in the cold against a given buffer and undissolved protein was removed by spinning in an Eppendorf micro centrifuge 5415D (F45-24-11 rotor) at 12,000 rpm for 1 min. For both Beckman and Diode Array spectrophotometers, the instruments were calibrated using deionized water (dH₂O) and the absorbance of both the dialysis buffer and the protein sample was measured at relevant wavelengths. Measurements were between 0.1-1.0 absorbance units (samples were diluted so that absorbances reading fall in this range). An extinction coefficient, ϵ_{280} 1 mg/ml, of 0.25 was used after correction for scatter by subtracting $1.5 \times A_{320}$. The molar mass of tropomyosin was taken to be 66,000 g/mole.

2.2.4.2 Nanodrop spectrophotometry

A Thermo Scientific Nanodrop 2000 spectrophotometer was used to determine the concentration of DNA. The instrument was first blanked using 2 μ l of nuclease free water and then the

absorbance of the sample was measured. The ratio of the two absorbance measurements at 260 and 280 nm indicated the nucleic acid purity of the sample.

2.2.4.3 Bradford Assay

The Bradford assay (Bradford, 1976) was used to determine the elution profile from affinity chromatography (see section 2.7). Column fractions (1 ml) were mixed carefully with 100 μ l of Bradford reagent (Bio-Rad) by gentle inversion. The absorbance at 595 nm was recorded using the Diode Array spectrophotometer. Column buffer (1 ml) was used to calibrate the instrument.

2.2.5 Gel Electrophoresis

SDS PAGE was performed according to the methods described by Laemmli (1970) using a 12% (w/v) acrylamide (Bio-Rad) separating gel. To prepare the gel, stock acrylamide solution (30% (w/v) acrylamide and 0.8% (w/v) bis acrylamide) was diluted with separating buffer (0.75 M Tris-HCl, 0.21% (w/v) SDS, pH 8.8) to a total volume of 20 ml. The solution was polymerized by adding 20 μ l N, N, N', N'- tetremethylethylenediamine (TEMED, Promega) and 100 μ l of 10% (w/v) ammonium persulfate solution (APS, Promega). Stacking gel was diluted to 3% (w/v) acrylamide from the stock solutions to a total volume of 5 ml and polymerized with 80 μ l APS and 6 μ l TEMED. A Bio-Rad Protean II apparatus was used for the electrophoresis sandwich. Gels were generally 7.0 cm long, 10.0 cm wide and 0.75 mm thick. Prior to loading onto the gel, protein samples were diluted at a ratio of 1:1 using 2x Laemmli buffer composed of 50 mM Tris-HCl, pH 6.8, 2% (w/v) SDS, 0.1% (w/v) bromophenol blue, 10% (v/v) glycerol and 2-5 mM dithiothreitol (freshly added). A volume of 10 μ l of Precision Plus Protein Unstained Standards (BioRad, cat # 161-0363, 10-250 kDa) was loaded into one of the lanes.

Electrophoresis was carried out at 180 V and stopped when the tracking dye ran off the gel. Gels were stained in 0.25% (w/v) Coomassie Brilliant Blue R-250 (BioRad), 50% (v/v) ethanol and 10% (v/v) acetic acid and then destained in 15% (v/v) acetic acid and 20% (v/v) ethanol.

2.3 Mutagenesis

2.3.1 Oligonucleotide primers

Custom made oligonucleotide primers were obtained from Operon (Huntsville, Alabama) and were used for the site directed mutagenesis:

T77K	5'	CTTGAGGTGGCTGAGAAGAAAGCCACGGAC	3'	FORWARD
Mutation	5'	GTCCGTGGCTTTTCTTCTCAGCCACCTCAAG	3'	FORWARD

The primers had a melting temperature of 71.5 °C. The underlined nucleotide is the one that differs from the original cDNA.

2.3.2 Purification of pTRC99A plasmid from E. coli BL21 cells

Unless otherwise stated, all centrifugation steps were performed in an Eppendorf microcentrifuge 5415D (F45-24-11 rotor) at room temperature. 60 µl of E. coli BL21 cells containing the expression vector pTRC99A (Pharmacia, 27-5007-01), which contains the Atlantic salmon fast skeletal muscle tropomyosin cDNA (Accession # NM_001123656) (Jackman *et al.*, 1996), was used to inoculate 6 ml of LB broth containing 25 µg/ml chloramphenicol and 100 µg/ml ampicillin and incubated overnight at 37 °C with agitation. The DNA from the overnight culture

was isolated using the Wizard Plus Miniprep kit (Promega) in accordance with manufacturer's instructions. Briefly, the cells were sedimented at 12,000 rpm for 2 mins and resuspended in 300 μ l of cell resuspension solution. Cell lysis solution (300 μ l) was added and sample was inverted several times. Neutralization solution (30 μ l) was added and again the sample was inverted several times. Samples were pelleted at 15,000 rpm for 10 mins and supernatant was purified using the resin provided in the kit. The mini-column was washed using the wash solution provided and by centrifugation at 12,000 rpm for 2 mins. Nuclease-free water (50 μ l) was used to elute the DNA and by a short centrifugation at 12,000 rpm.

2.3.3 Site-directed mutagenesis

Site-directed mutagenesis was carried out by means of the polymerase chain reaction using the QuickChange Lightning Site-Directed Mutagenesis kit (Stratagene). All reagents were provided in the kit. Briefly, double stranded DNA template (10-100 ng) was mixed with 5 μ l of 10 \times reaction buffer, 1 μ l of dNTP mix, 1.5 μ l of QuikSolution reagent and 125 ng of each of the two custom-made oligonucleotide primers (see section 2.3.1). The sample was diluted to a final volume of 50 μ l with sterile dH₂O and then 1 μ l of QuickChange Lightning enzyme was added. DNA was amplified using a MJ Research Peltier Thermal Cycler 200 machine using the following parameters:

Segment	Cycles	Temperature	Time
1	1	95 °C	2 minutes
2	18	95 °C	20 seconds
		60 °C	10 seconds
		68 °C	30 seconds/kb of plasmid length
3	1	68 °C	5 minutes

Following amplification, 2 μ l of *Dpn* I was added and the reaction mixture was incubated at 37 °C for 5 min.

2.3.4 Transformation of *E. coli* XL10-Gold Ultracompetent Cells

Beta-mercaptoethanol (2 μ l) was added to 45 μ l of XL10-Gold ultracompetent cells in a pre-chilled tube which were then incubated on ice for 2 min. 2 μ l of *Dpn* I treated reaction mixture (above) was added to the tubes which were incubated on ice for 30 min. After 30 min, tubes were heat pulsed in a 42 °C water bath for 30 sec followed by incubation on ice for 2 min. 0.5 ml of NZY+ broth (preheated in a water bath to 42 °C) was added to the mixtures and tubes were incubated at 37 °C for 1 hr with shaking. 100 and 200 μ l of the transformation mixtures were plated onto LB agar plates containing 25 μ g/ml chloramphenicol and 100 μ g/ml ampicillin. The

plates were incubated overnight at 37 °C. Following overnight incubation, a colony from the plate was used to inoculate 5 ml of LB broth containing 25 µg/ml chloramphenicol and 100 µg/ml ampicillin. The culture was incubated overnight at 37 °C with shaking.

2.3.5 Transformation of E. coli BL21 Cells

CaCl₂ (450 µl, 0.1 M) was added to 50 µl of competent E. coli BL21 cells in pre-chilled tubes. DNA (10-100 ng) was added and the sample was incubated on ice for 30 min. The sample was heat shocked for 60 sec at 42 °C and incubated on ice for 2 min. 900 µl of preheated (42 °C) Super Optimal broth with Catabolite repression (SOC) (Invitrogen) was added and the transformation reaction was incubated at 37 °C for 1 hr with shaking. The cells were concentrated by centrifugation at 12,000 rpm for 2 min and the entire transformation reaction was spread onto LB agar plates containing 25 µg/ml chloramphenicol and 100 µg/ml ampicillin. The plates were incubated overnight at 37 °C. A white colony was used to inoculate 10 ml of LB broth containing 25 µg/ml chloramphenicol and 100 µg/ml ampicillin. The cell culture was incubated at 37 °C overnight with continuous agitation and finally stored at -80 °C in equi-volume glycerol.

2.4 DNA Sequencing

Mutations were confirmed by DNA sequencing at CREAT, Genomics and Proteomics Facility, Memorial University of Newfoundland, Canada. The primers (from Operon) used to sequence the tropomyosin insert of the expression vector were:

M13/pUC reverse 5' AGCGGATAACAATTTTCACACAGG 3'

pBad-rev 5' ATCAGACCGCTTCTGCGTTC 3'

CREAIT uses an Applied Biosystems ABI3730x1 sequencer that is automated except for some preliminary set-up. For each sample, 2 μ l of 5x sequencing buffer, 0.5 μ l of sequencing mix, 3.2 pmol of a primer, DNA template (at least 500 pmol) and nuclease-free water to obtain a volume of 20 μ l was added at RT. Samples were mixed by vortexing briefly in a table top microcentrifuge. pGEM was set up as a control. A 9800 thermocycler (Applied Biosystems) was used for PCR amplification using the following program: 6 minutes at 96 °C, 25 cycles at 96 °C for 10 seconds each, 50 °C for 5 seconds, 60 °C for 4 minutes and then 4°C until the samples were removed from the thermocycler. The samples were again briefly centrifuged at RT. The Agencourt CleanSEQ system (Agencourt Bioscience) was used to purify the PCR product for sequencing. Briefly, 10 μ l of Agencourt CleanSEQ magnetic beads was added to each sample followed by 62 μ l of 85% ethanol (v/v) and mixed thoroughly. Samples were placed onto a magnetic plate (Agencourt SPRIPlate 69R). When the solution was clear (3-5 min), it was aspirated from the sample and discarded. A 100 μ l aliquot of 85% ethanol (v/v) was added to the sample and after 30 seconds, the ethanol was discarded. This ethanol wash was performed again and the sample left to air dry for 10 min. Deionized water (40 μ l) was added to the sample after which it was removed from the magnetic tray. After 5 min, the sample was returned to the magnetic tray to isolate the DNA. After 5 min, 35 μ l of sample was loaded into the ABI 3730x1 for sequencing. Sequencing results were analyzed using FinchTV from Geospiza and compared to the cDNA of Atlantic salmon fast muscle tropomyosin (Accession # NM_001123656).

2.5 Protein expression and isolation

Bacterial expression of the recombinant tropomyosin (mutated and non-mutated) was performed as described by Jackman *et al.* (1996). Briefly, 40 ml of LB broth containing 25 µg/ml chloramphenicol and 100 µg/ml ampicillin was inoculated with 400 µl of *E. coli* cells. The cell culture was incubated overnight at 37 °C with agitation. 4 L of LB broth containing 25 µg/ml chloramphenicol and 100 µg/ml ampicillin was inoculated with the 40 ml of overnight cell culture. The culture was incubated at 37 °C with shaking and the absorbance at 600 nm was monitored. When the absorbance reached 0.6 – 0.8, expression of tropomyosin was induced using 0.5 mM isopropyl β-D-thiogalactopyranoside (IPTG) (overnight, 37 °C, with shaking). The following morning, the cells were pelleted in a Beckman J6-HC centrifuge at 4,000 rpm and 4 °C for 20 minutes. The cells were dispersed in 100 ml of 0.2 M NaCl, 50 mM MOPS, 1 mM DTT at pH 7.0 and passed through a French pressure cell at room temperature (RT). The lysate was mixed with 1200 ml of the above buffer and stirred for 15 min (RT) following the addition of phenylmethylsulfonyl (PMSF) fluoride (saturated, in isopropanol). Samples were centrifuged at 4,000 rpm and 4 °C for 20 min. The supernatant was pH precipitated by adjusting the pH to 4.6 and centrifuged at 4,000 rpm and 4 °C for 30 min. The pellets were dispersed in 800 ml total of buffer (0.2 M NaCl, 50 mM Tris, 0.5 mM EDTA, 0.25 mM DTT pH 7.9) at ~10 °C for 15 min (again with addition of PMSF). Samples were centrifuged at 4,000 rpm and 4 °C for 20 min in a Beckman J6-HC centrifuge. The supernatant was precipitated by ammonium sulfate (45%) followed by centrifugation at 4,000 rpm and 4 °C for 30 min in a Beckman J6-HC centrifuge. Centrifugation was followed by 70% ammonium sulfate precipitation of the supernatant. The sample was then centrifuged at 8,000 rpm for 45 min in a Beckman J2-21 centrifuge (JA-10 rotor) at 4 °C. The pellets were dissolved in dH₂O and dialyzed against dH₂O (containing ammonium bicarbonate

and mercaptoethanol) in the cold for 2 days with 4 water changes (for a total of 20 L). Finally, the dialyzed sample was lyophilized.

2.6 Enrichment of Tropomyosin

2.6.1 Ion-Exchange Chromatography

Approximately 300 mg of protein was dissolved in 40 ml of filtered starting buffer of 75 mM NaCl, 30 mM Tris, 1 mM dithiothreitol, pH8.0, at 10 °C. A 2.5 x 14 cm Q Sepharose Fast Flow column (volume of ~ 70 ml) (GE Healthcare Biosciences) was equilibrated with ~300 ml of the above buffer (filtered) at a flow rate of ~15 ml/hr, in the cold room. The dissolved protein solution was centrifuged at 6,500 rpm for 11 minute; the supernatant was decanted and then loaded onto the column at a rate of ~ 20 ml/hr. The column was washed with ~ 100 ml of starting buffer, at the same rate. The protein was eluted from the column by a salt gradient (300 ml+300 ml) of 75 – 500 mM NaCl. Elution occurred at a rate of ~ 30 ml/hr and fractions were collected every 9 min using a LKB 7000A UltroRac fraction collector. The collected fractions were analyzed via absorbance at 280 nm and by conductivity measurements (CDM 80 conductivity meter, Radiometer) to determine which fractions contained tropomyosin. Fractions believed to contain tropomyosin were confirmed via SDS 12% PAGE.

2.6.2 Hydroxyapatite Chromatography

A 2.5 x 10 cm hydroxyapatite column (volume of ~ 50 ml) (Bio-Rad) was equilibrated at room temperature with 200 ml of filtered starting buffer containing 1 M NaCl, 0.01% NaN₃, 30 mM sodium phosphate, 1 mM dithiothreitol, pH 7.0 at a rate of ~15 ml/hr. The combined tropomyosin containing fractions from the Fast Q column were directly loaded onto the column

at 15 ml/hr. The column was then washed with ~100 ml of starting buffer. Protein was eluted with a sodium phosphate gradient (300 ml+300 ml) of 30 mM - 250 mM at a rate of ~ 20 ml/hr. Fractions were collected every 8 min using a LKB 7000A UltroRac fraction collector. SDS 12% PAGE and absorbance measurements at 280 nm were used to determine the tropomyosin containing fractions. These fractions were combined and dialyzed over two days against dH₂O (containing ammonium bicarbonate and mercaptoethanol) while changing the water four times (for a total of 20 L). The sample was then lyophilized. The enrichment of the protein was assessed by SDS 12% PAGE.

2.7 Affinity chromatography

Five grams of freeze dried CNBr-activated Sepharose 4B (GE Healthcare, Biosciences) was re-suspended in 1 mM HCl to a final volume of 20 ml. The swollen gel was washed for 15 minute with 1 mM HCl (200 ml/g of powder) and filtered until semidry. The ligand (10 mg/ml troponin from rabbit skeletal muscle) dissolved in 20 ml of coupling buffer (0.1 M NaHCO₃, 0.5 M NaCl, pH 8.3) was mixed with the gel and rotated overnight at 4 °C. It was washed with 100 ml coupling buffer to get rid of excess ligand and any remaining active groups were blocked with 0.1 M Tris-HCl, pH 8 for 16 hours at 4 °C. The next step was to wash the Sepharose (containing immobilised troponin) with three cycles of alternating pH, each consisting of a wash with 0.5 M NaCl, 0.1 M acetate, pH 4 buffer followed by 0.5 M NaCl, 0.1 M Tris, pH 8 buffer. Finally the affinity medium was stored at 4 °C in the presence of 0.01% NaN₃ until packed into columns.

Samples (either mutant or non-mutant tropomyosin) were applied to the column (0.9 cm×6 cm) containing the ligand equilibrated in a start buffer containing 10 mM imidazole, 20 mM NaCl, 0.5 mM EGTA, 0.5 mM dithiothreitol, 0.01% NaN₃, pH 7, at 4 °C. Elution was effected by a

linear gradient (50 ml+50 ml) of 20-500 mM NaCl at a rate of 12 ml/hr. Protein detection was by Bradford assay and Coomassie R-250 staining of SDS polyacrylamide gels. The NaCl concentrations of fractions were obtained by measuring the conductivity (Radiometer Copenhagen, CDM 80 conductivity meter and CDC 114 electrode) and then converting into molarity using a standard curve generated for conductivity versus NaCl concentration.

2.8 Thermal stability studies

2.8.1 Circular dichroism

Approximately 10 mg of freeze-dried tropomyosin (either mutated or non-mutated) was dissolved in 2 ml of buffer (0.1 M KCl, 20 mM potassium phosphate, 0.01% NaN₃, 1 mM EGTA, 1.5 mM dithiothreitol, pH 7.0) and dialysed overnight against 1 L of the buffer in the cold room. Following dialysis, the sample was centrifuged to remove any insoluble protein. A protein concentration of either 1 or 2 mg/ml sample was used. Spectra were recorded using a Jasco 810 spectropolarimeter. Heat induced unfolding of mutant and non-mutant tropomyosins was determined by heating the protein from 5 °C to 70 °C in a water jacketed cell of 0.1 mm light path length and monitoring the ellipticity change at 222 nm. The temperature was controlled by a CTC-345 circulating water bath. The temperature increase was performed at a rate of 1 °C/min. The scanning speed of the instrument was set at 100 nm/min with normal sensitivity. The melting temperature was obtained by determining the temperature of the normalized data at 50% unfolding.

2.8.2 Differential scanning calorimetry

Unfolding of tropomyosin was studied using a NANO DSC (TA instrument) high sensitivity differential scanning calorimeter. Heat capacity profiles were obtained by increasing the temperature at a rate of 1 °C/min. Samples were dialysed against 2 ml buffer (0.1 M KCl, 20 mM potassium phosphate, 0.01% NaN₃, 1 mM EGTA, 1.5 mM dithiothreitol, pH 7.0) in the cold overnight. Approximately 800 ul buffer and sample (mutant or non-mutant recombinant tropomyosin, 2-3 mg/ml) was loaded to reference and sample cells respectively. A temperature gradient of 5-70 °C was used as per the circular dichroism experiments. For a single sample, at least three cycles of heating, cooling, and reheating was performed.

2.9 Proteolytic methods

2.9.1 Chymotrypsin and trypsin digestion

Limited proteolysis by chymotrypsin and trypsin were carried out as described by Pato *et al.* (1981). The enzyme (2 mg) was dissolved in 2 mM HCl and dialyzed (10 mm dialysis tubing) overnight. Generally, 10 mg of tropomyosin was dissolved in 2 ml of buffer: 50 mM NH₄HCO₃, 0.1 M NaCl, 1 mM DTT, pH 8.5. The protein was dialyzed (10 mm dialysis tubing) overnight against 1L of buffer in the cold room. Tropomyosin (400 µg) was digested with 0.6 µg of chymotrypsin (Worthington Biochemical Corporation) or trypsin (Sigma, Aldrich) (~1:500 enzyme to substrate mole ratio) at room temperature for 30 minute. At intervals, 20 µl of reaction mixture was removed and inhibited using 1 µM lima bean trypsin inhibitor (Worthington Biochemical Corporation) (dissolved in 20 mM Tris, pH 7.5). Digestion patterns were analyzed on a SDS 12% PAGE.

2.10 Electroblotting of digested samples

Western blotting was performed on the proteolytic digest of mutant recombinant tropomyosin as described by Heeley and Hong (1994). The protein was transferred from unstained SDS-polyacrylamide gels to polyvinylidene difluoride membrane in a mini-Trans-Blot Electrophoresis Transfer cell (Bio-Rad). Blotting was carried out in a buffer of 10 mM CAPS (N-cyclohexyl-3-aminopropanesulfonic acid), 10% (v/v) methanol, pH 11.00 at 60 V for 3 hrs. The membrane was briefly stained (2 min) in 40 % (v/v) methanol, 0.1% Coomassie Brilliant Blue R-250 and destained in 50% (v/v) methanol (< 5 min). The membrane was then left to air dry. Edman-based sequencing was performed in the Advanced Protein Technology Center at Sick Children's Hospital, Toronto.

2.11 Data manipulation

2.11.1 cDNA sequences

All cDNA sequences were analyzed using FlinchTV (Geospiza) to perform blast searches and visualize electrograms.

2.11.2 Graphing

Graphing was done using Graphpad Prism.

Chapter 3

Results and Discussion

3.1 Purification of DNA from BL21 Plasmids

The pTrc99A expression vector with tropomyosin cDNA insert from the E. Coli BL21 cells was used to express sufficient quantities of recombinant tropomyosin for biochemical analysis. The concentration was assessed by using a Nanodrop (Thermo scientific) spectrophotometer. The Nanodrop gives the ratio for the measurements of A260/A280, which indicates the nucleic acid purity. A value between 2.0 – 2.2 indicates an acceptable level of protein content. The DNA samples that were used had an A260/A280 ratio of 1.8-2.1. The concentrations of the DNA were determined to be between 80-120 ng/μl.

3.2 Deoxyribonucleic Acid Sequencing

The mutation of the tropomyosin at position '77' was confirmed prior to any experimental analysis. The nucleotide sequencing was carried out in CREAT and the sequence results were compared to that of *Salmo salar* (Atlantic salmon) fast myotomal muscle tropomyosin mRNA (Accession # NM_001123656). Six candidates of the mutant tropomyosin were submitted for sequencing and only the samples (five of six) that contained the desired mutated nucleotide base were used for further experiments. Figure 5 shows the mutation from threonine (ACA) to lysine (AAA) at position 231.

3.3 Expression of Tropomyosin

Isopropyl β -D-1 thiogalactopyranoside (IPTG) (500 μ M) was used to induce the expression of tropomyosin from cultures of *E. coli* BL21 cells. Small scale (approximately 8 ml of bacterial culture) induction of tropomyosin (Figure 6) was carried out prior to large scale (4 L) induction to ensure that the tropomyosin would be expressed. In the case of the non-mutant (control), the electrophoretic analysis of a total cell lysate (Figure 6, right-sided gel) shows that tropomyosin is one of the major protein components (Figure 6, right-side gel, centre lane). Conversely, the appearance of an induced protein band is not clearly evident in the case of the Thr77Lys mutant (Figure 6, left-sided gel). This can be explained by an alteration in the electrophoretic mobility of the mutant rather than a lack of induction for the following reasons. When protein was isolated from an induced lysate by isoelectric-precipitation and subjected to SDS PAGE but with 5 M urea in the separating phase (Sender, 1971), which is a well-known test for tropomyosin, a band migrating at approximately 55,000 Da was observed (data not shown) which was not seen in Figure 6, signifying the presence of tropomyosin (Sender, 1971). Further, from close inspection of the stained gel in Figure 6 it is evident that the bacterial protein band positioned just below the 37,000 Da marker is more intensely stained in the induced mutant sample compared to the uninduced sample. This would arise if the electrophoretic mobility of Thr77Lys tropomyosin in the presence of SDS (and with no urea in the separating phase) is increased relative to the control, a point that is substantiated later in the thesis, such that the mutant runs together with this particular bacterial protein.

Such shifts in tropomyosin have been reported before, the classic case being the separation of the alpha and beta isoforms in rabbit skeletal muscle (Cummins and Perry, 1973). Based on amino acid sequence information (Mak *et al.*, 1980) it has been hypothesized that the presence of additional positively charged groups in tropomyosin leads to the binding of more detergent molecules rather than any difference in shape.

Tropomyosin is not the only protein to display anomalous migration during SDS PAGE. Other examples include proteins that contain a large number of aspartates and glutamates (Matagne *et al.*, 1991), carbohydrate (Grefrath and Reynolds, 1974) and hydrophobic residues (Rath *et al.*, 2009). In these instances the mass ratio of SDS to protein varies from the value of 1.4 g per g (Reynolds and Tanford, 1970). The present findings were useful in that they cater for the identification of fragments containing Lys77 (see section 3.6).

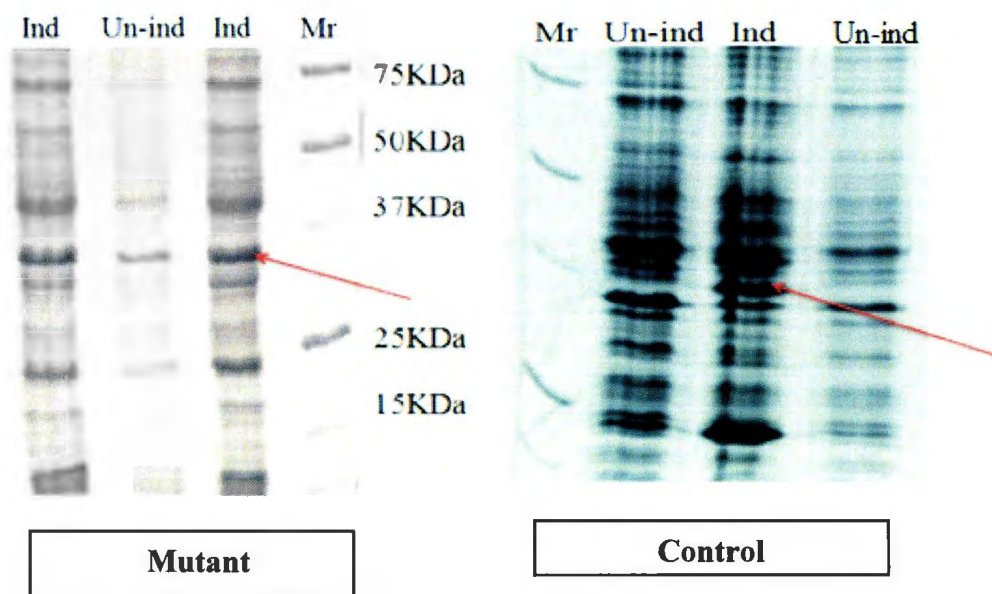


Figure 6: SDS PAGE analysis of a lysate of IPTG-induced E. coli BL21 cells containing recombinant tropomyosins

Five ml of LB broth (containing 25 $\mu\text{g/ml}$ of chloramphenicol and 100 $\mu\text{g/ml}$ of ampicillin) was inoculated using 5 μl of E. coli BL21 cells. The samples were induced with 500 μM IPTG when the A_{600} was between 0.6-0.8 and then incubated overnight at 37 $^{\circ}\text{C}$. 100 μl of sample was pelleted and dissolved in 50 μl of SDS buffer. 10 μl of sample was run on 12% (w/v) SDS polyacrylamide gel and stained in Coomassie Brilliant Blue R-250. Mutant contained the Thr77Lys mutation, non-mutant recombinant tropomyosin was used as control. 'Ind' represents induced cultures, 'Un-ind' represents un-induced cultures, Mr is a molecular weight marker; arrows point to the induced tropomyosin in both control and mutant samples.

Enrichment of tropomyosin was carried out on a large scale by isoelectric point precipitation and salt-induced precipitation followed by ion exchange and hydroxyapatite chromatography. Figure 7 shows the elution profile of protein from a Q Sepharose Fast Flow column with a salt gradient of 75-500 mM NaCl. Fractions were analysed via absorbance at 280 nm and electrophoresis (Figure 7 and 8 insets) confirmed that the protein was eluting in fractions 171-193. These fractions were pooled and loaded directly onto a hydroxyapatite column. This column works because negatively charged groups within tropomyosin are adsorbed by Ca^{2+} sites and then eluted by a phosphate gradient (30-250 mM phosphate). Tropomyosin eluted in fractions 121-150 (Figure 8) were pooled, dialyzed against dH_2O and lyophilized. The level of enrichment of the final sample was assessed by SDS PAGE using loadings of $>10 \mu\text{g}$ (Figure 9). At such a high loading a few trace contaminants are evident, but it is clear that the main component of the protein samples is tropomyosin. The yield was $\sim 20 \text{ mg}$ of enriched tropomyosin per litre of growth medium. A final point is that Figure 9 demonstrates the mutant protein (lanes 2 and 3) to possess a slightly faster electrophoretic mobility than the non-mutant (lane 1). This shift causes the mutant to co-migrate with a bacterial protein making it harder to detect in a whole cell lysate (Figure 6).

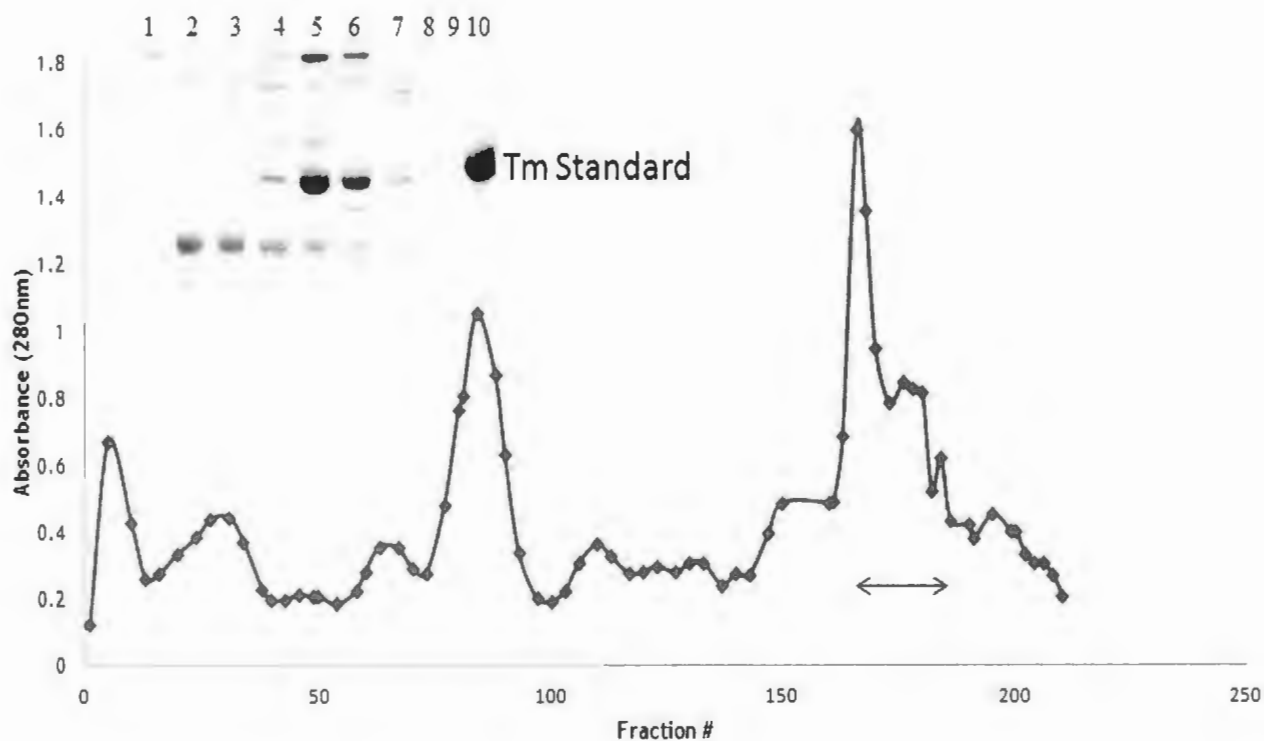


Figure 7: Q Sepharose Fast Flow chromatography profile of crude recombinant tropomyosin

Column dimensions, 2.5 x 14 cm (volume, 70 ml); buffer, 30 mM Tris, 1 mM DTT, pH8.0; salt gradient, 75-500 mM NaCl; cold room. Absorbance was measured at 280 nm using a Beckman DU-64 spectrophotometer. Horizontal bar indicates tropomyosin containing fractions as confirmed by SDS PAGE (inset). Lane numbers 1-9 correspond to fraction numbers 84, 110, 166, 173, 176, 178, 182, 190, and 195, respectively. Lane 10 is tropomyosin standard. Tropomyosin band was more intense at fraction number 176.

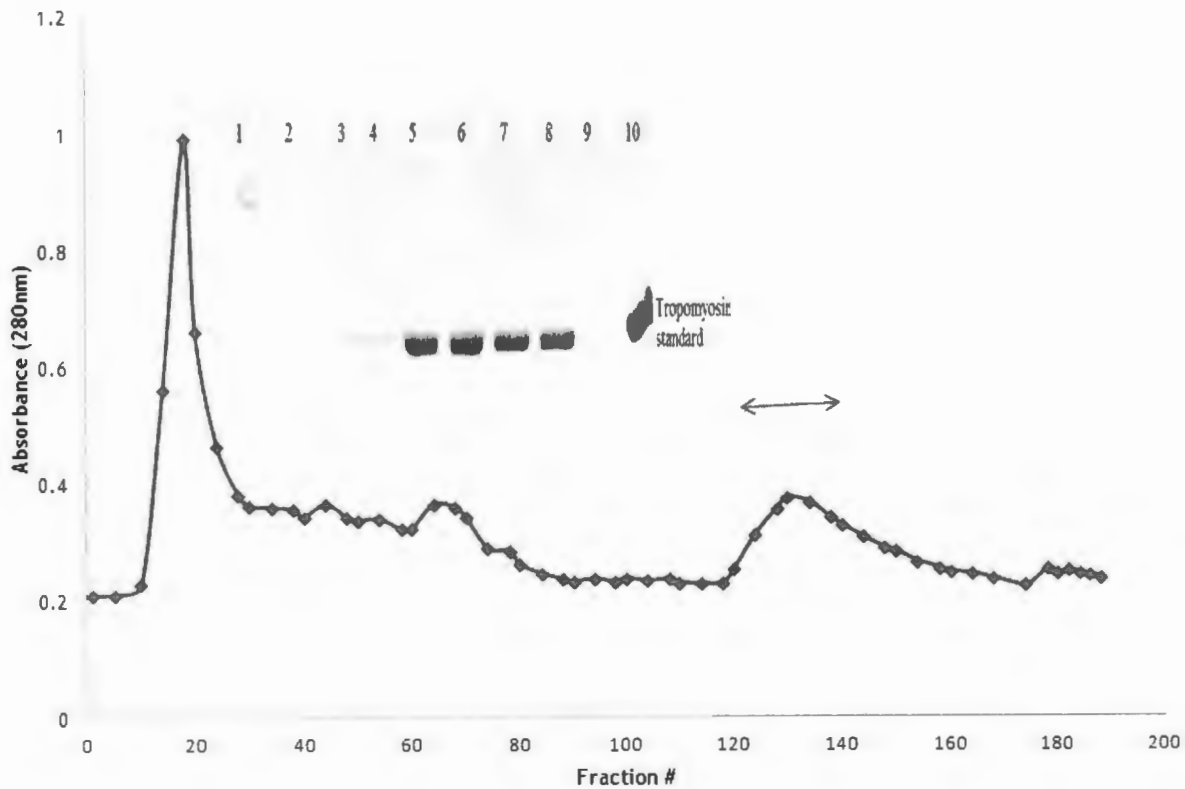


Figure 8: Hydroxyapatite chromatography profile of recombinant tropomyosin

Column dimensions, 2.5 x 16 cm (volume, 80 ml); buffer, 1 M NaCl, 0.01% NaN₃, 1 mM DTT, pH 7.0; phosphate gradient, 30-250 mM sodium phosphate; temperature, ~25 °C. Fractions 121-150 contained tropomyosin (indicated by a horizontal bar) as assessed on SDS gel (inset). Lane numbers 1-9 correspond to fraction numbers 18, 64, 115, 120, 124, 128, 134, 138, and 148, respectively. Lane 10 is tropomyosin standard.

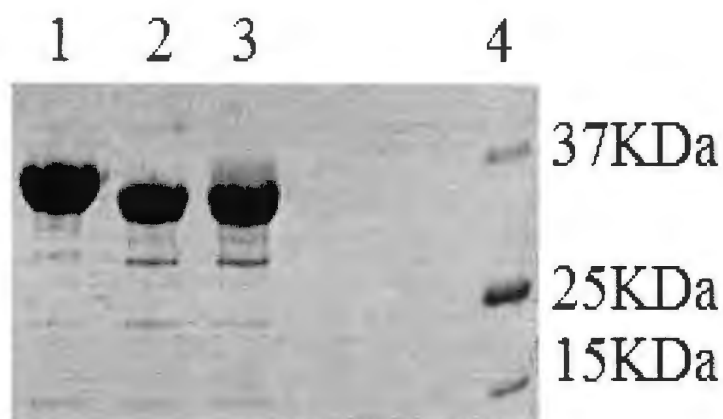


Figure 9: SDS PAGE analysis of highly-enriched mutant and non-mutant tropomyosins

1 – Non-mutant recombinant tropomyosin; 2 and 3 – two loadings of Thr77Lys mutant recombinant tropomyosin; 4 – Molecular weight markers. More than 10 ug of protein was loaded into lanes 1-3. Lane 4 contained molecular weight markers. The 12% (w/v) polyacrylamide gel was stained in Coomassie Brilliant Blue R-250.

3.4 Thermal stability studies

3.4.1 Circular dichroism

Figures 10 to 16 document the use of circular dichroism (CD) to observe the heat-induced unfolding of the mutant and non-mutant recombinant tropomyosin (~ 2 mg/ml in 0.1M KCl, 20 mM potassium phosphate, 1.5 mM DTT, 0.01% NaN₃, pH 7.00). Unfolding profiles were developed by monitoring the ellipticity at 222 nm as a function of temperature. The signal at 222 nm is sensitive to the α -helical content of the molecule (Greenfield and Fasman, 1969). This wavelength was chosen because it is well known that the secondary structural elements of tropomyosin are mainly α -helical (Cohen and Szent-Gyorgyi, 1957). The samples were exposed to temperatures from 5-70 °C, at a rate of 1 °C / min. The average of the first 4 data points (5-9 °C) was taken to be the starting (100%) ellipticity and the average of the last 4 data points (67-70 °C) was taken to be the end (0%) ellipticity. Each sample was analyzed at least five times and the results were averaged in order to create a normalized melting curve of the samples. The formula used to calculate the normalization was:

$$\frac{\theta - \theta_{\text{end}}}{\theta_{\text{start}} - \theta_{\text{end}}} \times 100$$

Where: θ is the ellipticity of the sample at the particular temperature

θ_{end} is the average ending ellipticity and

θ_{start} is the average starting ellipticity

The melting temperature (T_m) was taken to be the temperature at which there was a 50% signal change. The change in relative ellipticity at 222 nm as a function of temperature showed that the

transition temperature for unfolding of non-mutant and mutant tropomyosin are 40 °C and 45 °C (Figures 10 and 13), respectively, at 0.1 M salt (pH 7 + DTT) when heated at a rate of 1 °C/min, indicating that non-mutant tropomyosin is the least conformationally stable of the two (Table 2).

Since there is only a single amino acid difference between the two tropomyosins this reduction in melting temperature is directly attributable to the presence of threonine in position 77 (as opposed to lysine). Comparing the 20 amino acid differences among salmon and rabbit tropomyosins (Table 1), the mutation of threonine (salmon) to lysine (rabbit) occurs at a 'g' position which, as mentioned earlier, is important for salt bridge formation. On this point the salmon protein may (compared to rabbit) lose an intra-helical ion pair (between Lys-77 and Asp-80) as well as an inter-helical ion pair (between Lys-77 and Glu-82) (Figure 2A).

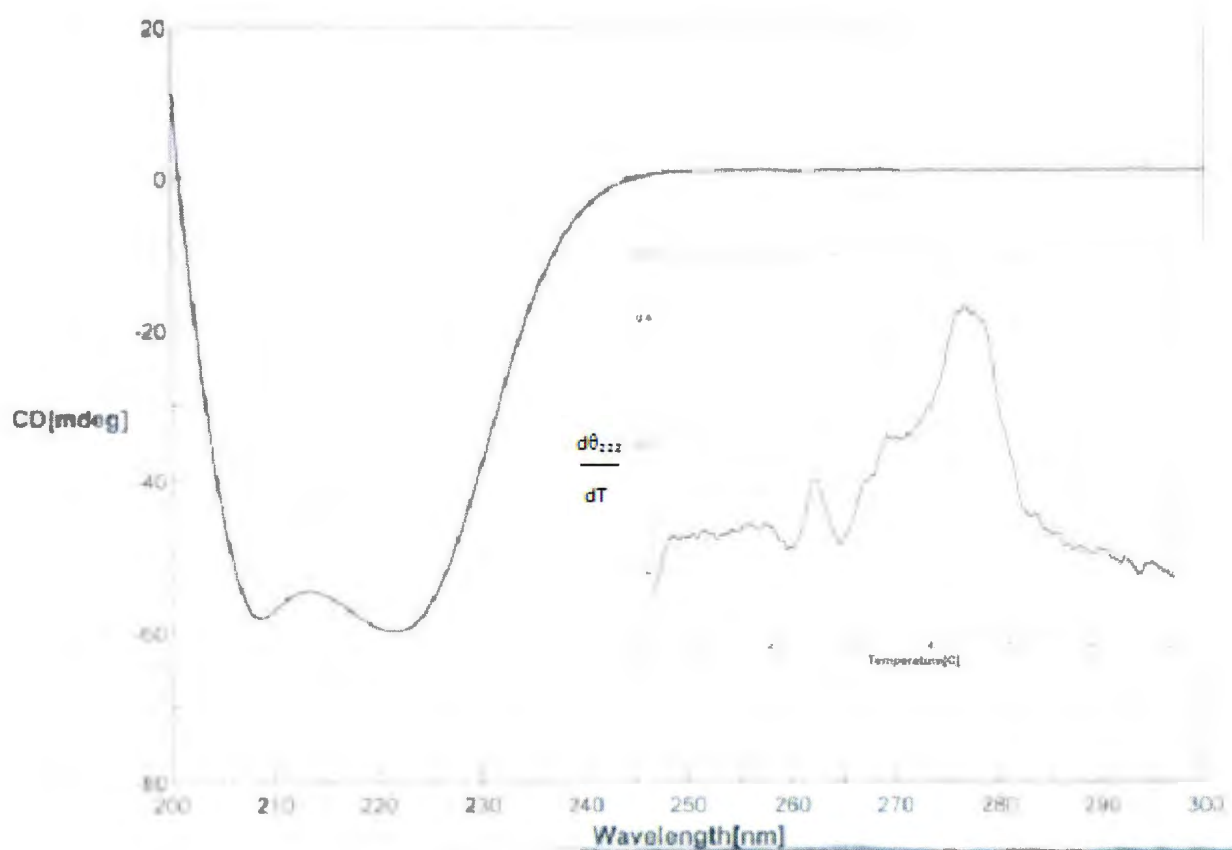


Figure 10: Circular dichroism and thermally induced unfolding of the Thr77Lys mutant recombinant tropomyosin from Atlantic salmon

Ellipticity of mutant tropomyosin ($\sim 2\text{mg/ml}$ in 0.1M KCl , 20mM potassium phosphate, 1.5mM DTT, 0.01% NaN_3 , $\text{pH } 7.00$) at 222nm was monitored constantly over a linear temperature gradient of $5\text{-}70\text{ }^\circ\text{C}$ using a Jasco-810 spectropolarimeter. Heating rate was at $60\text{ }^\circ\text{C}$ per hour and light path length, 0.1mm . Main graph is a wavelength scan at $5\text{ }^\circ\text{C}$. Inset is the first derivative of the ellipticity change monitored at 222nm over the temperature gradient. Average melting temperature of five repeated experiments is $45\text{ }^\circ\text{C} \pm 0.2$.

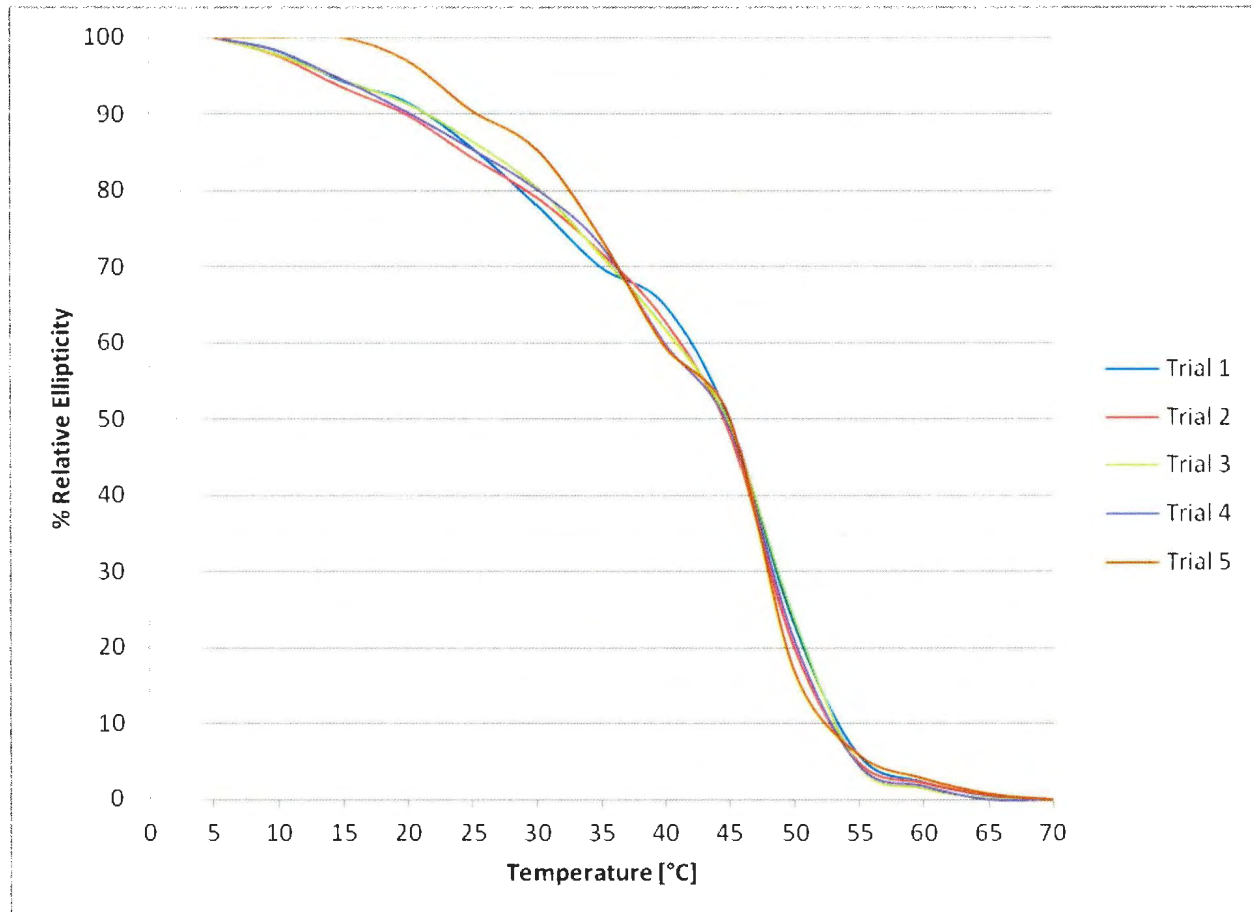


Figure 11: Normalized curve of the melting profiles of five samples of Thr77Lys

Unfolding was monitored at 222 nm from 5-70 °C in a 0.1 mm cell. Five samples of tropomyosin from the same stock (2 mg/ml in 0.1 M KCl, 20 mM potassium phosphate, 0.01% NaN₃, 1 mM EGTA, 1.5 mM DTT pH 7.0) were analysed. The first three trials were performed on a freshly dialyzed material. The last two trials were performed the next day on frozen sample. There was no detectable difference between the trials on the two different days.

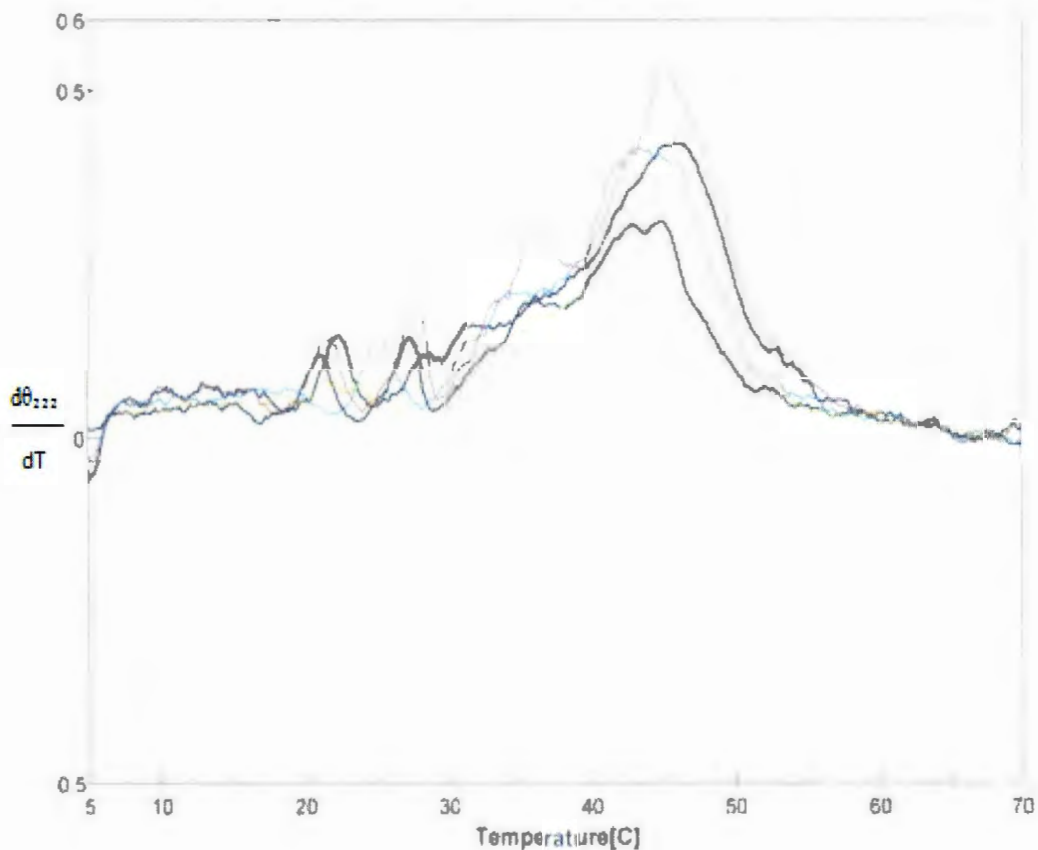


Figure 12: Thermally induced unfolding of the Thr77Lys mutant recombinant tropomyosin from Atlantic salmon as monitored by far-UV circular dichroism.

First order derivative of ellipticity of mutant tropomyosin (~2mg/ml in 0.1M KCl, 20mM potassium phosphate, 1.5mM DTT, 0.01% NaN₃, pH 7.00) as monitored at 222nm over a linear temperature gradient of 5-70 °C using a Jasco-810 spectropolarimeter. Heating rate was at 1 °C per minute and light path length, 0.1mm. The melting experiments were repeated at least five times with an average melting temperature of 45 °C ± 0.2. Partial unfolding, in the twenty degree range, of salmon fast tropomyosin has been observed before (Jackman et al 1996). However, the above traces are too noisy for a firm conclusion to be made.

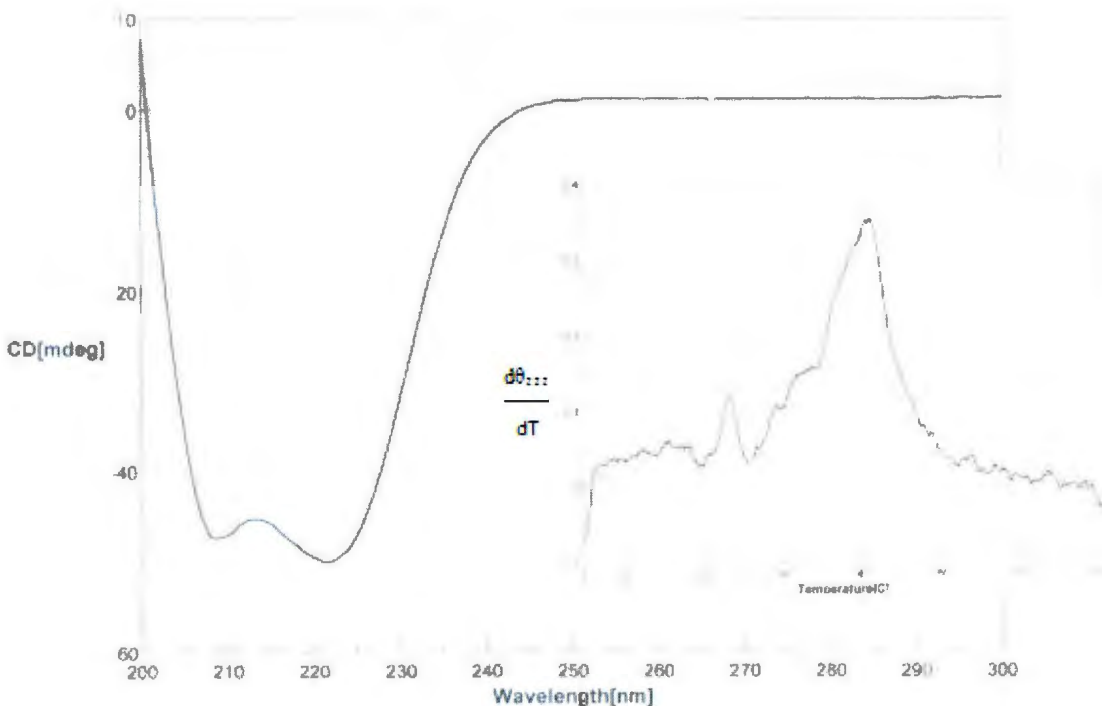


Figure 13: Circular dichroism and thermally induced unfolding of the non-mutant recombinant tropomyosin from Atlantic salmon

Ellipticity of mutant tropomyosin (~2mg/ml in 0.1M KCl, 20mM potassium phosphate, 1.5mM DTT, 0.01% NaN₃, pH 7.00) at 222nm was monitored constantly over a linear temperature gradient of 5-70 °C using a Jasco-810 spectropolarimeter. Heating rate was at 1 °C per minute and light path length, 0.1mm. Main graph is a wavelength scan at 5 °C. Inset is the first derivative of the ellipticity change monitored at 222nm over the temperature gradient. The average melting temperature of five repeated experiments is 40 °C ± 0.24.

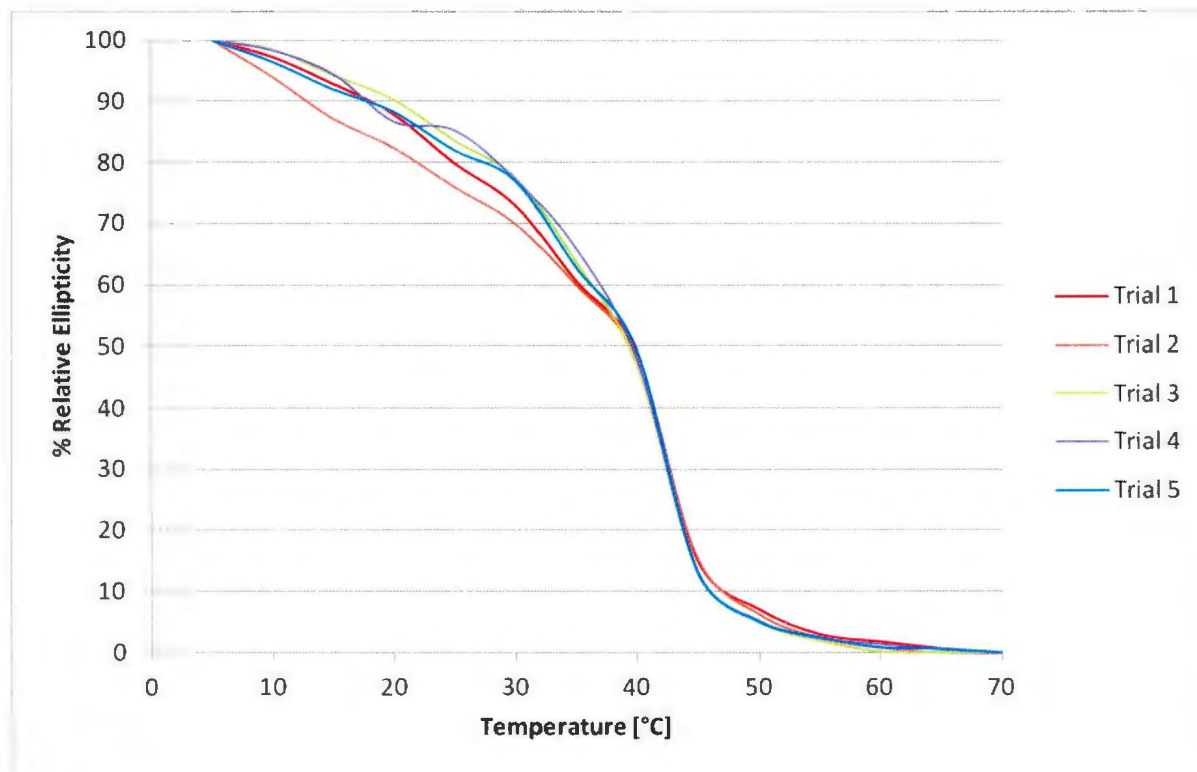


Figure 14: Normalized curve of the melting profiles of five samples of non-mutant recombinant tropomyosin

Unfolding was monitored at 222 nm from 5-70 °C in a 0.1 mm cell. Tropomyosin sample, 2 mg/ml, in 0.1 M KCl, 20 mM potassium phosphate, 0.01% NaN₃, 1 mM EGTA , 1.5 mM DTT, pH 7.0

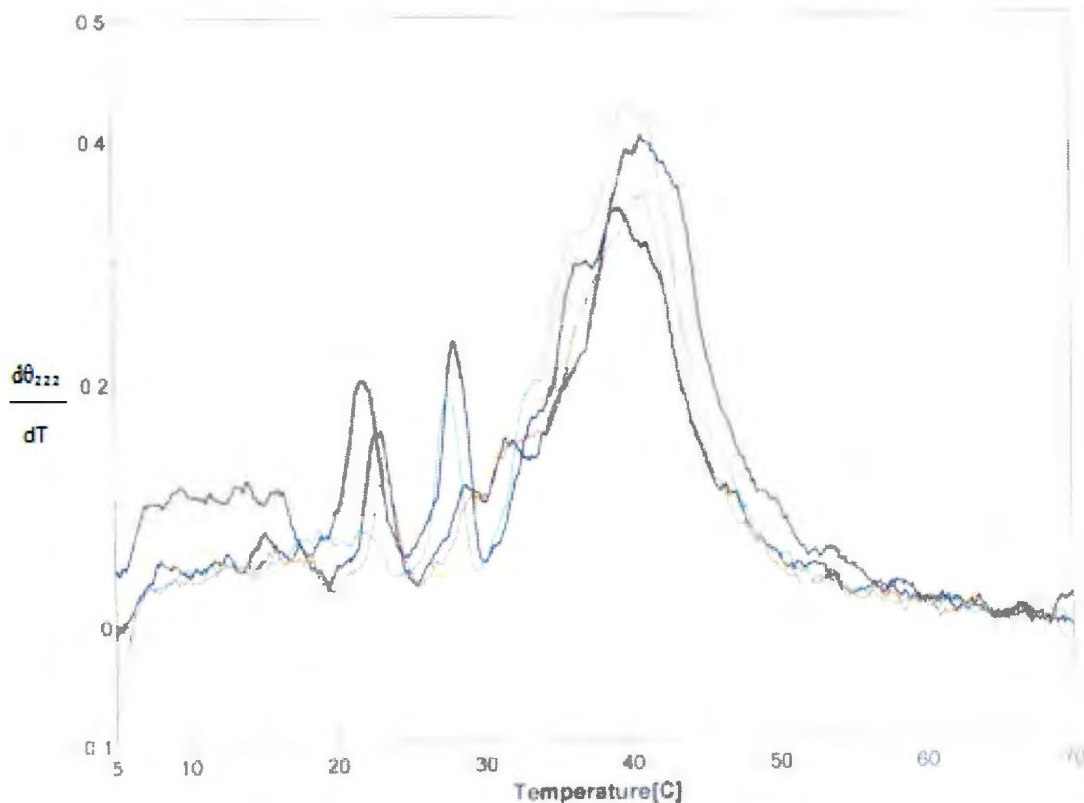


Figure 15: Thermally induced unfolding of the non-mutant recombinant tropomyosin from Atlantic salmon as monitored by far-UV circular dichroism.

First order derivative of ellipticity of non-mutant tropomyosin (~2mg/ml in 0.1M KCl, 20mM K (P), 1.5mM DTT, 0.01% NaN₃, pH 7.00) as monitored at 222nm over a linear temperature gradient of 5-70 °C using a Jasco-810 spectropolarimeter. Heating rate was at 1 °C per minute and light path length, 0.1mm. The melting experiments were repeated at least five times with an average melting temperature of 40 °C ± 0.24. As with Figure 12, on account of the noise we are cautious about attributing the peaks in the twenty degree range to an unfolding event.

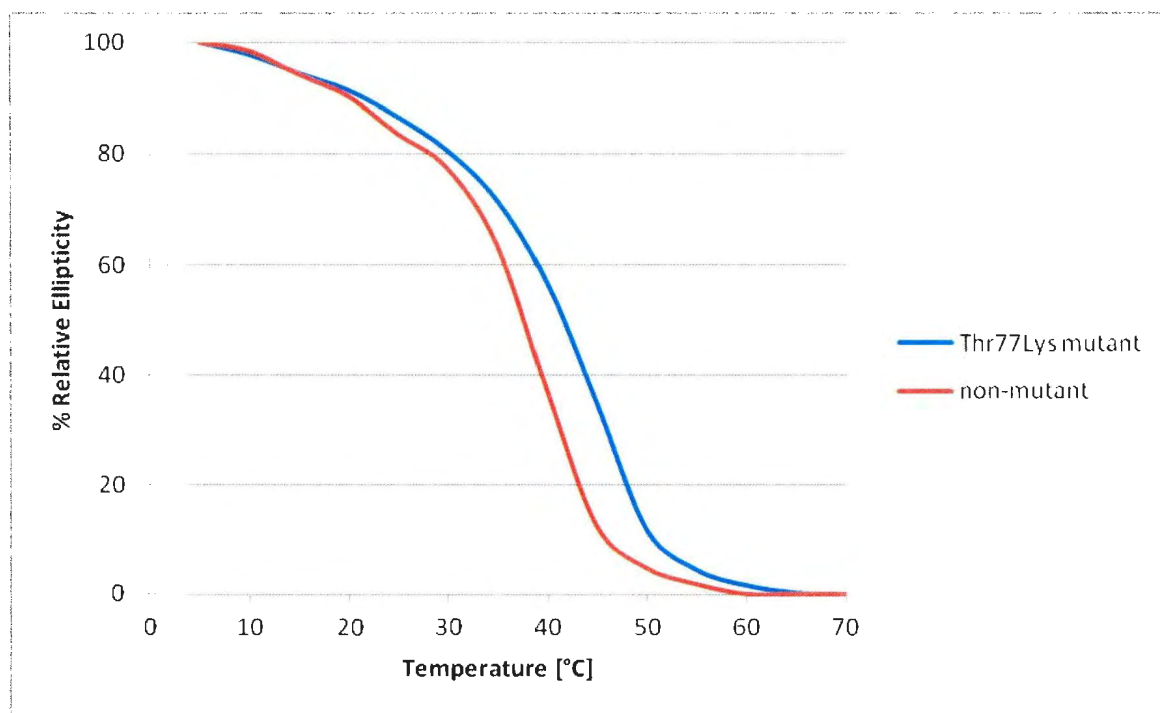


Figure 16: Comparison of the averaged, normalized melting curves of the mutant and the non-mutant tropomyosin.

The curves are colour coded: Mutant Thr77Lys in blue, non-mutant in red.

3.4.2 Differential scanning calorimetry

A calorimeter was used to monitor the thermal denaturation of non-mutant and mutant recombinant tropomyosin by direct heating (Figure 17 and 18). This procedure was carried out in order to corroborate the results obtained using circular dichroism. Calorimetry was conducted with protein solutions at a concentration (5 mg/ml) higher than those used for circular dichroism (2 mg/ml) but the same buffer composition and pH (7.00) was used for both experiments. The melting temperatures of non-mutant and mutant tropomyosin were determined to be 40.5 and 43.5 °C respectively. Thus, like circular dichroism, calorimetry indicates that the mutant is less thermally stable. An unfolding study of rabbit and shark tropomyosins by Hayley *et al.* (2011) also revealed agreement between the two methods, indicating that the change in secondary structure measured by circular dichroism and the overall thermodynamic phase change measured by calorimetry are not independent events.

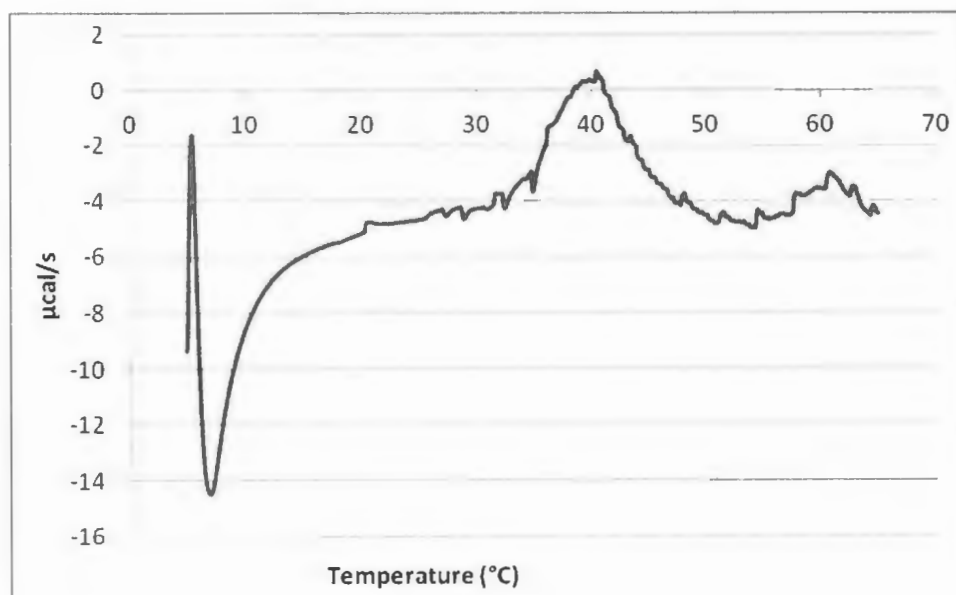


Figure 17: Thermal denaturation of non-mutant recombinant tropomyosin as monitored by differential scanning calorimetry.

Experimental details are as follows: protein concentration, 5 mg/ml; buffer, 0.1 M KCl, 20 mM phosphate, 1.5 mM DTT, 0.01% NaN₃, pH 7.00; scan rate, 1 °C/min; cell volume, 0.3 ml.

Exothermic heat of reaction profiles is presented as the first derivative of the progressive curve versus temperature. Melting temperature, 40.5 °C.

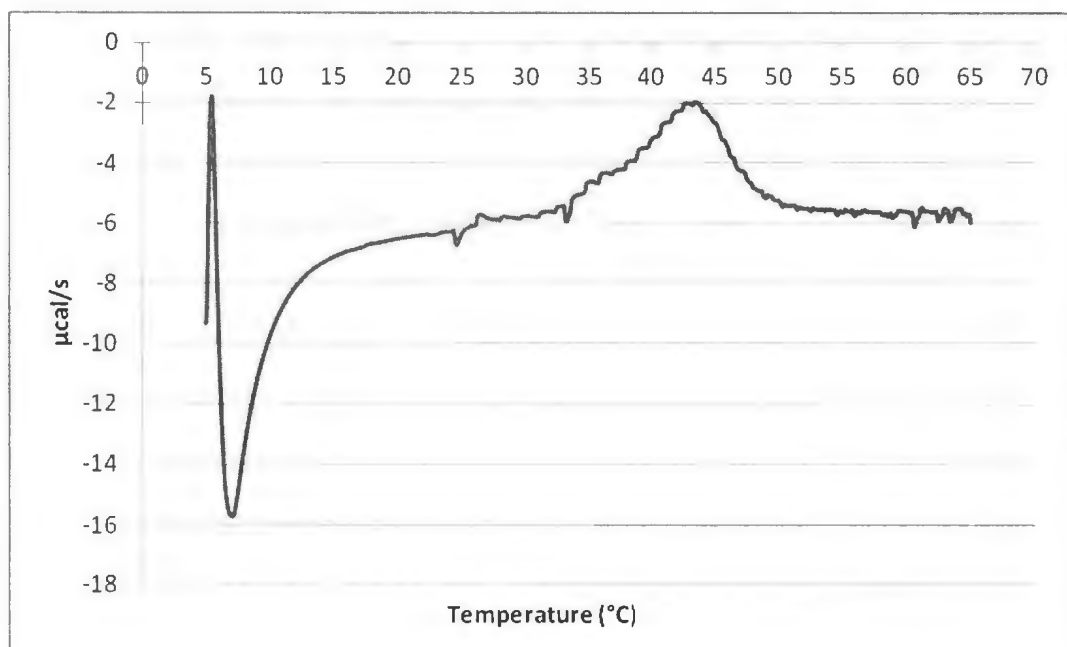


Figure 18: Thermal denaturation of mutant recombinant tropomyosin as monitored by differential scanning calorimetry.

Experimental details are as indicated in Figure 17. Melting temperature, 43.5 $^{\circ}\text{C}$.

3.5 Affinity Chromatography

3.5.1 Effect of T77K mutation on the binding of tropomyosin to troponin

The binding affinity of mutant and non-mutant recombinant tropomyosin to troponin was assessed on troponin-Sepharose 4B using a linear gradient of sodium chloride. Protein elution was determined by Bradford assay of the chromatography fractions and Coomassie R-250 staining of electrophoretically separated protein bands. Figures 19 and 20 show the elution profiles and conductivity measurements. At a loading of ~15 nmoles both recombinant tropomyosins bound to the column. The affinities of interaction were compared by taking the conductivity reading of the fraction having the highest absorbance. When this was done, it is evident that the non-mutant eluted earlier in the salt gradient than the mutant. The conductivities are: non-mutant, 4.3 mS/cm (Figure 19) and mutant, 6.5 mS/cm (Figure 20). Using a NaCl standard plot, these conductivities correspond to NaCl concentrations of 30 and 55 mM (Table 2). Thus, under the experimental conditions used, the mutation of threonine to lysine at position 77 in the amino acid sequence can be said to enhance adhesion of tropomyosin to its thin filament partner, troponin.

There are a number of published reports (Brisson *et al.*, 1986; White *et al.*, 1987; Goonasekara *et al.*, 2007, and Goonasekara and Heeley, 2009) which point to the existence of a troponin-T binding site within the amino-terminal region of tropomyosin such that troponin-T forms a 'bridge' across the overlap site. On the surface, the current findings are consistent with this postulate but there are a number of complicating factors. One, due to the difficulty in preparing troponin from fish (D. Heeley, personal communication), the source of the immobilised troponin

was rabbit skeletal muscle. It follows that a different result may have occurred with the true physiological form of troponin. Two, since tropomyosin can be likened to a protein transmission cable, the consequence of the mutation, while not grossly altering the structure, may not be restricted to the locality of residue-77. That is, there could well be ramifications for the downstream and up-stream flanking parts of the molecule. Three, unacetylated tropomyosin is expected to be essentially monomeric (i.e. non-polymerised) even in the low ionic strength chromatography start buffer. If troponin-T attaches to sequences at either end of tropomyosin, a mixture of interactions can be envisaged. On this point, a simpler future experiment would be to use the cyanogen bromide fragment of troponin-T (res. 1 – 151) in conjunction with tropomyosin-Sepharose. Either way, it would not be possible to rule out a non-specific charge effect involving clusters of negative charges in troponin-T (Pearlstone *et al.*, 1977 a and b) as the basis for the altered interaction (Figures 19 and 20). Further, it should be noted that the loss of the amino-terminal acetyl group has a big negative effect on troponin-T binding (Palm *et al.*, 2003 and Goonasekara *et al.*, 2007).

Despite the limitations of the chromatography method which was used in this research project, the results represent a start and provide sufficient grounds to warrant further investigation.

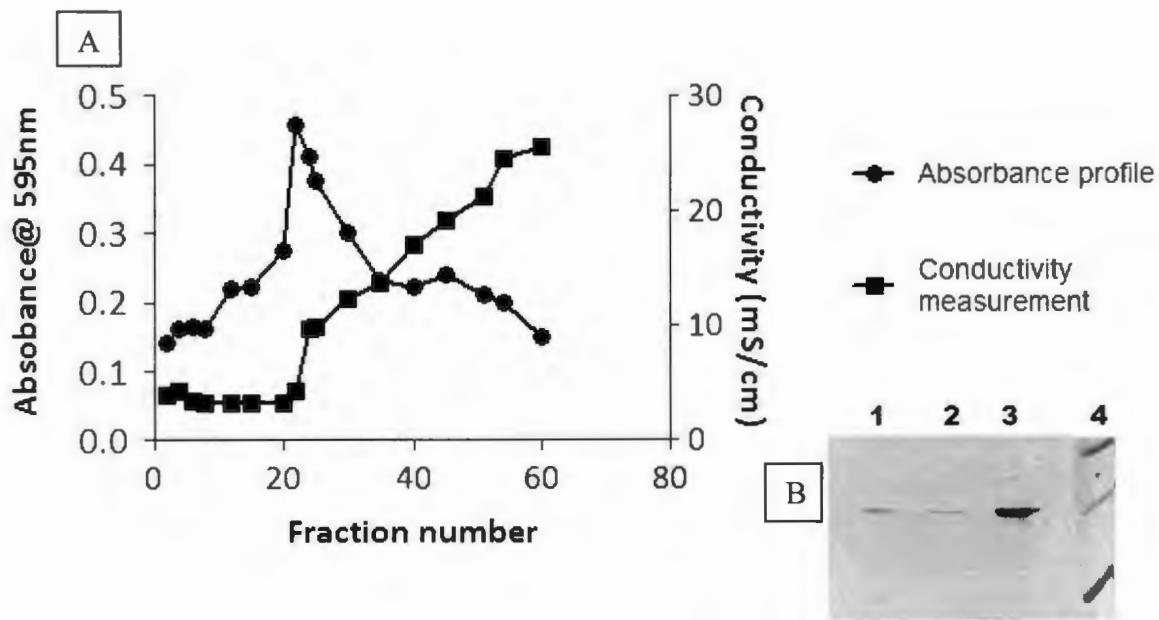


Figure 19: Affinity chromatography profile of non-mutant recombinant tropomyosin

Buffer: 10 mM imidazole, 0.5 mM DTT, 0.5 mM EGTA, 0.01% NaN₃, pH 7 in cold room with a NaCl gradient of 20 to 500 mM. Column dimensions, 1 cm (width) x 6 cm (length); fraction volume, 1.2 ml; flow rate, 0.2 ml/min; amount of tropomyosin loaded, ~1 mg (15 nanomoles). Protein detection was by Bradford assay (A_{595}) (Panel A) and Coomassie R-250 staining of SDS polyacrylamide gels (Panel B).

B: SDS PAGE of eluted fractions. Lane 1-3 with fraction numbers 12, 20, and 22 and molecular weight marker (lane 4) of about 10 μ l were loaded on the gel after heating mixture of eluted sample (50 μ l) and sample buffer (50 μ l). Binding affinity is apparent from the intensity of the stained bands as a function of fraction numbers.

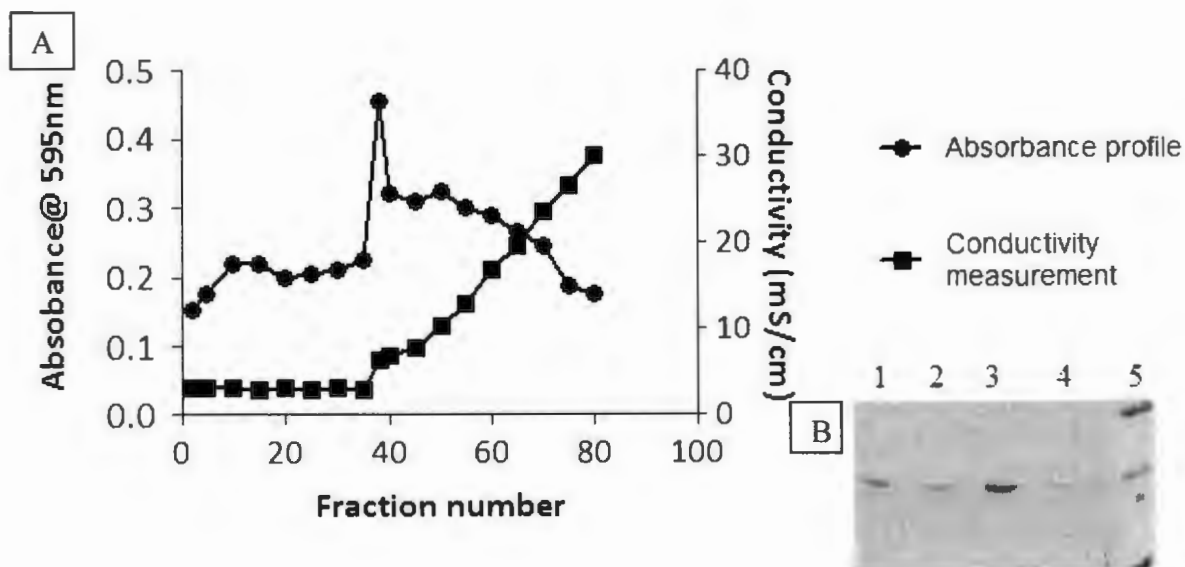


Figure 20: Affinity chromatography profile of mutant T77K recombinant tropomyosin

The experimental conditions were the same as mentioned in Figure 19.

B: SDS PAGE of eluted fractions. Lane 1-4 with fraction numbers 25, 35, 38, and 42 and molecular weight marker (lane 5) of about 10 μ l were loaded on the gel after heating mixture of eluted sample (50 μ l) and sample buffer (50 μ l). Binding affinity is apparent from the intensity of the stained bands as a function of fraction numbers.

Table 2: Comparison of mutant and non-mutant tropomyosin

	Affinity Chromatography (mM)	Circular Dichroism (T °C)	Differential Scanning Calorimetry (T °C)
Control	30	40±0.24	40.5
Mutant T77K	55	45±0.2	43.5

- Affinity chromatography: The NaCl concentration (mM) corresponds to the chromatography fraction containing the greatest amount of tropomyosin as determined by Bradford assay and staining of polyacrylamide gel.
- Circular dichroism: The temperature corresponds to the mid-point of the θ_{222} versus temperature unfolding profile. Standard deviation \pm .
- Differential scanning calorimetry: Exothermic heat of reaction profiles versus temperature.

3.6 Proteolytic analysis

3.6.1 Chymotrypsin and trypsin digestion

Limited proteolysis was used to examine the effect that a threonine at position 77 has on the conformational stability of Atlantic salmon tropomyosin compared to lysine in the same position, as occurs in rabbit tropomyosin. Chymotrypsin cleaves peptide bonds on the carboxy-terminal side of phenylalanine, tyrosine and tryptophan and sometimes leucine and methionine. The initial cleavage site of chymotrypsin in rabbit tropomyosin is residue 169 (leucine) (Pato and Smillie, 1981). Trypsin cleaves peptide bonds on the carboxy-terminal side of lysine and arginine.

Time studies were performed at a temperature of 25 °C. Digestion was halted by addition of a protein inhibitor followed immediately by heating in SDS-containing buffer. The time samples were then applied to the same gel (Figures 21 and 22) whereupon, after electrophoresis and staining, the shifted mobility of mutant Thr77Lys is once more evident. In the case of chymotrypsin (Figure 21) the first proteolytic product, observed after 10 minute incubation, runs just under the band corresponding to intact protein (Figure 21, lanes 3 and 4). This result indicates that the preferred site of cleavage involves the removal of a short peptide from one of the ends of the molecule leading to a small change in mobility. Judging from the staining intensities (Figure 21, lane 3 and 4), at the ten minute mark roughly 50% cleavage has occurred at the preferred site in both tropomyosins. At this stage in the experiment no fragments are observed farther down the gel (Figure 21 lane 3 and 4) but continued incubation leads to the appearance of smaller fragments, apparent masses ~15 kDa and ~12 kDa (Figure 21, lanes 5 – 8). Based on their sizes, it can be assumed that these polypeptides emanate from cleavage within the

centre of the molecule. In addition to the smaller pieces, the later time samples also contain the long fragment but no intact protein.

Interestingly, the ~15kDa polypeptide exhibits the mobility-shift that has been described earlier, but the ~12 kDa polypeptide does not (Figure 21, lanes 5 – 8). A simple interpretation is that the larger of these two fragments contains residue 77 and the smaller represents the carboxy-terminal portion which is of equivalent length (mutant and non-mutant). Another observation is that there is no dramatic difference in susceptibility of the two tropomyosins to chymotrypsin, although the two smaller fragments are present in greater abundance based on their darker staining (and the intact molecule is in correspondingly lower abundance) in the mutant compared to the non-mutant (see lanes 7 and 8 of Figure 21). Thus, it is possible that the Thr77Lys is slightly more susceptible to proteolysis in the middle of the molecule than the control.

When the experiment is repeated with trypsin it is clear that mutation of residue 77 does not markedly alter the timing pattern of digestion (Figure 22). The outcome of treatment with trypsin is more complicated than with chymotrypsin in that more fragments are generated. From previous work (Goonasekara *et al.*, 2008) one of these is expected to arise from cleavage within the triple lysine sequence between residues 5 – 7. Such an event is consistent with the band in lanes 5 and 6 of Figure 22 positioned under the one corresponding to full-length protein. At the earliest time sampled of 5 minutes, four major fragments are detected in the middle of the gel (Figure 22, lanes 3 and 4). The mobility of two of these species is shifted (mutant versus non-mutant), suggesting that they contain residue-77 whereas the other two are not shifted. In terms of susceptibility to trypsin, the mutant tropomyosin appears to be breaking down at a slightly

faster rate relative to the control, but as in the chymotrypsin experiment the difference is not dramatic.



Figure 21: Comparison of the susceptibility of mutant T77K and non-mutant tropomyosins to limited chymotryptic digestion at room temperature.

Buffer: 50 mM NH_4HCO_3 , 0.1 M NaCl, 1 mM DTT, pH 8.5. 400 μg tropomyosin digested with 0.6 μg chymotrypsin (~ 1:500 enzyme to substrate mole ratio). The reaction was stopped by mixing with lima bean trypsin inhibitor. Samples were heated in the presence of SDS, electrophoresed and stained using Coomassie R-250. The two tropomyosins were digested side-by-side.

Mutant T77K – Lanes 1, 3, 5, and 7. Non-mutant – Lanes 2, 4, 6, and 8. Lane 10- Molecular weight marker. Lanes 1 and 2 have no chymotrypsin and the ensuing lanes represent increasing intervals of time (10, 20, and 30 minutes.)

The fragments that were sequenced following western blotting are indicated as 1, 2, and 3.

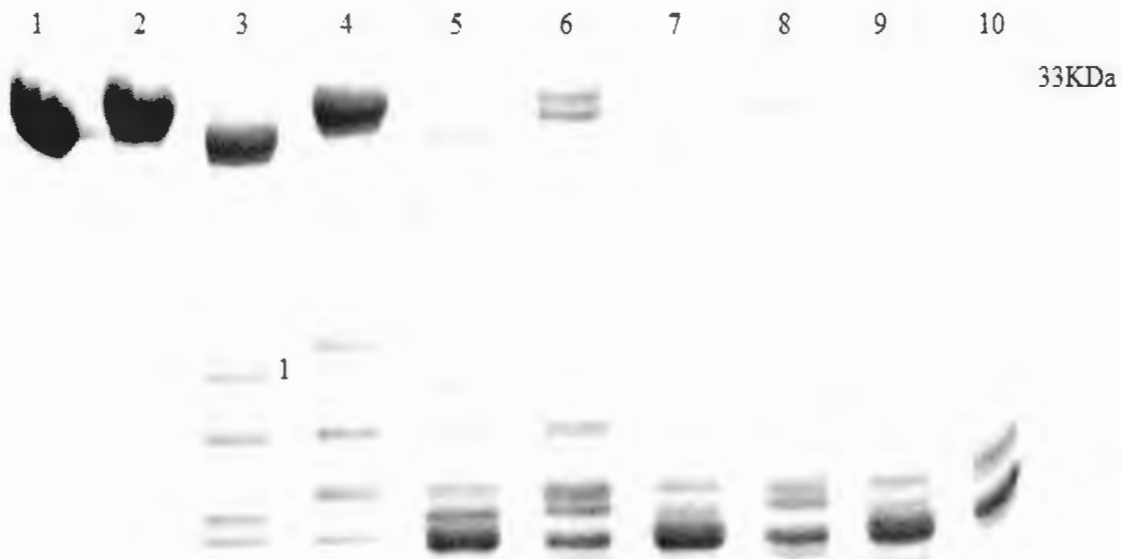


Figure 22: Comparison of the susceptibility of mutant T77K and non-mutant tropomyosins to limited tryptic digestion at room temperature.

The experimental conditions were the same as mentioned in figure 22.

Mutant T77K – Lanes 1, 3, 5, 7, and 9. Non-mutant – Lanes 2, 4, 6, 8, and 10. Lanes 1 and 2 have no chymotrypsin and the ensuing lanes represent increasing intervals of time (5, 15 30 and 60 minutes). Only one fragment (1) was sequenced.

3.7 Sequencing of Proteolytic Fragments

Aliquots of the samples from the proteolysis experiment (Figures 22 and 23) were also electroblotted with a view to performing Edman-based sequencing. Three fragments from the chymotrypsin digestion and one from the trypsin digestion were selected. For chymotrypsin, fragment 1 (as indicated in Figure 22 lane 4) was the large fragment from non-mutant tropomyosin. It was subjected to 11 cycles of sequencing. Fragments 2 and 3 (as indicated in Figure 22 lane 5) from mutant tropomyosin each underwent 6 sequencing cycles. For trypsin, only one fragment was sequenced (as indicated in Figure 23) from mutant tropomyosin. It underwent 6 cycles as well. The results are summarised in Table 3.

Table 3: Amino-terminal sequences of electroblotted fragments of recombinant Atlantic salmon tropomyosin.

Chymotrypsin
Fragment 1: Lys ₁₂ -Leu-Asp-Lys-Glu-Asn-Ala-Leu-Asp-Arg-Ala ₂₂
Fragment 2: Lys ₁₂ -Leu-Asp-Lys-Glu-Asn ₁₇
Fragment 3: Val ₁₇₀ -Ile-Ile-Glu-Ser-Leu ₁₇₅
Trypsin
Fragment 1: Met ₁ -X-Ala-Ile-Lys-Lys ₆

The partial sequences were aligned with the published sequence of Atlantic salmon fast muscle tropomyosin (Heeley *et al.*, 1995). X, unidentified phenylthiohydantoin amino acid.

Comparison with the complete sequence of salmon skeletal tropomyosin (Heeley *et al.*, 1995), demonstrates that the amino-terminal residue for chymotryptic fragments 1 and 2 is Lys12. Since fragment 1 is the first proteolysed product (Figure 21), this shows that the initial chymotrypsin cleavage site on recombinant salmon tropomyosin (using a temperature of 25 °C) is the peptide bond between residues Leu11 and Lys12. Further, since there is no reported evidence of chymotrypsin cleaving close to the carboxy-terminal end of the molecule, the large fragment can be assumed to encompass residues 12 – 284. The initial internal cleavage site in the mutant tropomyosin was not determined by sequencing but appears to be the same as the non-mutant. This statement is based on the fact that the distance on the gel (Figure 21) between the large fragment and the corresponding intact protein is the same for both tropomyosins.

The mutation at position 77 had no detectable effect on hydrolysis of the peptide bond between Leu-11 and Lys-12. Figure 21 shows that following 10 minutes of digestion (lanes 3 and 4) the two samples of tropomyosins had roughly equal amounts of the large fragment. Although chymotrypsin usually cleaves proteins on the carboxy-terminal side of aromatic amino acids, it occasionally cleaves on the carboxy-terminal side of leucine. The same is true for rabbit skeletal tropomyosin, however, in the case of the mammalian protein a different leucine is involved, residue 169 (Pato and Smillie, 1981). Interestingly this particular leucine occurs at the N-terminus of fragment 3 (Table 3). Since this fragment is produced after fragment 1 in the time study (Figure 21), Leu-169 is considered a secondary cleavage site in recombinant tropomyosin.

Thus, putting all of the evidence together, the first product of chymotryptic digestion is a large fragment spanning residues 12 – 284 and a smaller fragment that ran off the gel. Subsequent cleavage of this fragment yields two fragments, residues 12 – 168 (fragment 2) and residues 169 – 284 (fragment 3). It should be pointed out that fragment 2, which contains the mutated amino acid, displays a mobility shift whereas fragment 3 does not (Figure 21).

What is the reason for the different action of chymotrypsin on skeletal tropomyosins from fish and mammal? One possible explanation is that the recombinant tropomyosin is unacetylated. Research has shown that having an unacetylated methionine at residue 1 causes the protein to be more destabilized at the N-terminus (Hitchcock-DeGregori and Heald, 1987; Greenfield *et al.*, 1994; Frye *et al.*, 2010). This destabilization could be the reason as to why the recombinant salmon tropomyosin is initially cleaved by chymotrypsin near the N-terminus. A second possible explanation for the difference in initial cleavage is the presence of a unique pair of glycines at positions '24' and '27' in salmon tropomyosin which makes it more flexible and thus more susceptible to proteolysis (Fudge and Heeley 2011).

The tryptic fragment (Figure 22) that was selected for sequencing gave methionine in the first cycle (Table 3). Although it was not possible to assign an amino acid in second cycle, the subsequent cycles show that this fragment contains the first six amino acids in tropomyosin (Table 3). This is an important result because it demonstrates that the mutant tropomyosin is intact at this end.

Chapter 4

General Discussion and Future Experiments

4.1 General Discussion

Molecular motion is temperature-dependent. In the absence of compensation, large biomolecules such as proteins becomes excessively rigid at low temperature and cease to function.

Investigations of the strategies which prevent this from happening have been carried out mostly on globular proteins. Structural comparisons across different temperature regimes have revealed that no two protein families are exactly alike in how they deal with the cold. However, certain trends are apparent. In general, the number of intermolecular interactions decreases with decreasing growth temperature. For example, compared to the mesophilic (e.g. mammals and birds) and thermophilic homologues, proteins from psychrophilic organisms (growth temperature, lower than 15 °C) may possess fewer ion pairs and hydrogen bonds, a smaller hydrophobic contact area and larger loops (Greaves and Warwicker, 2009; Greaves and Warwicker, 2007; Gianese *et al.*, 2002). In comparisons of amino acid composition and sequence, psychrophilic proteins may contain, in critical regions, alanine in place of valine and more proline and glycine compared to the counterparts that operate at higher temperature.

Less is known about how rod-shaped proteins deal with cold. In view of the changes in physical position on the thin filament which it undergoes during contraction and relaxation, adaptation to cold is of direct relevance to tropomyosin. In the wild, the salmonidae (salmon, trout, and char)

are pelagic species, inhabiting the top 200 meters of the ocean column. They are cold-blooded; body temperature depends upon that of the environment. The Atlantic ocean hovers around the 10 °C mark with seasonal fluctuations making it somewhat warmer in the summer and somewhat cooler in the winter. In fresh water, which salmon return to in order to spawn, temperatures are higher but still far below 37 °C. Under such thermal conditions, how does salmon tropomyosin acquire adequate flexibility so that it can serve as an effective regulator of muscle activity?

Work performed in this laboratory has started to document flexibility-enhancing (cold-combative) characteristics within tropomyosin. For example, shark skeletal tropomyosin (twenty substitutions compared to rabbit-alpha skeletal) contains three closely-spaced core residues having a more hydrophilic amino acid than what occurs in the counterpart from mammal (Hayley *et al.*, 2008). These substitutions which occur at positions 179 (d), 190 (a) and 211 (a), were proposed to collectively reduce the conformational stability (i.e. increase flexibility) of a section that spans two thirds of the molecule in shark (Hayley *et al.*, 2011). In the case of Atlantic salmon fast muscle tropomyosin, Thr-179 (which is conserved in shark) and a unique pair of glycines present at positions 24 and 27 have been investigated by mutagenesis (Fudge and Heeley, 2011). Changing these residues to alanine increased stability either globally, as determined by circular dichroism or locally, as determined by limited proteolysis. These data demonstrate that greater flexibility is conferred on tropomyosin by the presence of polar side-chains within the hydrophobic seam of the coiled-coil and increasing the number of glycines, strategies that have been documented in globular proteins.

In this current work a third strategy to increase flexibility has been identified which centers on the interaction between a pair of oppositely charged side-chains. As stated above, proteins including tropomyosin from psychrophilic sources tend to contain a smaller number of ionic interactions compared to mesophiles (Greaves and Warwicker, 2009). Replacement of Thr-77 in salmon with the corresponding residue (lysine) in rabbit resulted in an increase in resistance to heat denaturation (Table 2). From this it can be stated that the amino acid at position 77 in salmon tropomyosin is destabilizing compared to that in rabbit.

What can be said about the relative contributions of each class of substitution – (i) polarity of coiled coil interface, (ii) glycine content and (iii) ion pair? Some information can be obtained by comparing the effects of various mutations. Compared to the respective control, mutations directed at (i) and (iii) shifted the melting temperature to a greater extent (by between 3 and 5 °C) than those aimed at (ii). Replacing the two glycines with alanines, yielded a smaller such change, one which bordered on experimental error (Fudge and Heeley, 2011). It would appear therefore that the loss of an ion pair at position 77 of salmon tropomyosin is similar in consequence to inserting an hydroxyl side-chain in the hydrophobic seam at position 179, at least when the melting temperature is measured by circular dichroism. Thus, it appears that the unique conformational properties of salmon tropomyosin stem from the adjustment of a variety of structural forces.

Finally, what advantage is there in salmon in having a neutral amino acid at residue 77 ('g')? The answer to the question may lie in the presence of clusters of 'core' alanines which occur in specific regions along tropomyosin. On account of alanine having a small side chain, these clusters have been proposed to create bends in the molecule allowing it to wind around filamentous actin (Brown *et al.*, 2001). Alternatively, the methyl group may produce local destabilization (Singh and Hitchcock-DeGregori, 2003), relative to larger non-polar residues in the same position. In both instances the outcome is the same: to permit formation of the actin-tropomyosin complex. Interestingly, the second actin binding period contains three 'core' alanines at 74, 78, and 81 residues which are conserved in salmon tropomyosin. Further, mutation of the alanines to amino acids with larger side-chains, Leu and Val, increases thermal stability and weakens actin affinity (Singh and Hitchcock-DeGregori, 2003). The current findings are consistent with the stability theory of Singh and Hitchcock-DeGregori (2003), in that the presence of a threonine instead of lysine in the middle of an alanine cluster causes further destabilization of this region of the molecule. We propose that Thr-77 occurs in salmon tropomyosin due to the need to maintain the 'proper' interaction with actin at low temperature. It is also possible that the interaction with troponin may be altered as implicated by the results of affinity chromatography (Figures 19 and 20). Either way, we conclude that this particular threonine is part of an adaptive strategy for the effective operation of fast skeletal muscle in the cold waters such as the Atlantic Ocean.

4.2 Future Experiments

Site-directed Mutagenesis.

The conformational properties of salmon tropomyosin could be further explored by mutating the Thr77Lys mutant which was engineered in the current study. Specifically, one or both of the carboxylic side-chains at positions 80 and 82 could be exchanged for alanine. A double mutation removing both of the negative charges is practicable given the closeness of the two groups in the sequence. Characterization of these new mutants, using the methodologies described in the thesis, would provide information on the network of ionic interactions occurring in this part of the molecule.

The effect of the Thr77Lys mutation on the interaction of tropomyosin with actin

Investigating the effect of the T77K mutation on the interaction of tropomyosin with actin will reveal if the amino acid is essential for actin binding. The interaction between tropomyosin and actin can be studied by sedimentation in an ultracentrifuge. However, in this instance a requirement would be to express the protein in a eukaryotic cell line so that the tropomyosin is acetylated, because as stated early in this thesis unacetylated tropomyosin binds weakly to actin (Hitchcock-DeGregori and Heald 1987). Alternatively a short (unacetylated) peptide could be fused to the bacterially-expressed protein in order to restore end-to-end polymerisation and actin affinity (Monteiro *et al.*, 1994).

Characterisation of cyanogen bromide fragments

Like other vertebrate striated muscle tropomyosins, Atlantic salmon tropomyosin can be cleaved with CNBr according to the method of Gross (1967) into two long peptides which are largely representative of each half of the protein, namely, residues 11-127 and 142-281. Characterization of the fragment containing the Thr77Lys mutation, using circular dichroism and limited proteolysis, would allow investigation of the effects of this substitution upon the conformational stability of tropomyosin's amino-terminal half. The expectation is that a larger shift in T_m would be observed for the isolated fragment compared to intact tropomyosin.

References

Alexander R.M. (2003) "Muscle, the motor" in Principles of Animal Locomotion. *Princeton, NJ: Princeton Univ Press*, pp. 15-34

Amphlett G.W., Syska H., Perry S.V. (1976) The polymorphic forms of tropomyosin and troponin I in developing rabbit skeletal muscle. *FEBS Lett.* 63: 22–26

Bailey K. (1946) Tropomyosin: a new asymmetric protein component of muscle. *Nature* 157: 368-369

Bone Q., Marshall N.B. (1982) Osmoregulation and ion balance. In: Biology of fishes. *Chapman & Hall, New York*, pp. 107–129

Bradford M.M. (1976) A rapid and sensitive method for the quantitation of microgram quantities of protein utilizing the principle of protein-dye binding. *Anal. Biochem.* 72: 248-254

Brisson J.R., Golosinska K., Smillie L.B., Sykes B.D. (1986) Interaction of tropomyosin and troponin T: a proton nuclear magnetic resonance study. *Biochemistry* 25: 4548-4555

Brown J.H., Kim K-H., Jun G., Greenfield N.J., Dominguez R., Volkman N., Hitchcock-DeGregori S.E., Cohen C. (2001) Deciphering the design of the tropomyosin molecule. *Proc. Natl. Acad. Sci.* 98: 8496 – 8501.

Brown J.H., Zhou Z., Reshetnikova L., Robinson H., Yammani R.D., Tobacman L.S., Cohen, C. (2005). Structure of the mid-region of tropomyosin: Bending and binding sites for actin. *Proc. Natl. Acad. Sci.* 102: 18878-18883

Butters C.A., Willadsen K.A. and Tobacman L.S. (1993) Cooperative interactions between adjacent troponin-tropomyosin complexes may be transmitted through the actin filament. *J. Biol. Chem.* 268: 15565 – 15570

Cohen C., Longley W. (1966) Tropomyosin paracrystals formed by divalent cations. *Science* 152: 794–796.

Cohen C., Szent-Gyorgyi A.G. (1957) Optical rotation and helical polypeptide chain configuration in α -proteins. *J. Am. Chem. Soc.* 79: 248-248 (Single page article)

Cohen C., Caspar D.L.D., Johnson J.P., Nauss K., Margossian S.S., Parry D.A.D. (1972) "Tropomyosin-Troponin Assembly." *Cold spring harbor symp. Quant. Biol.* 37: 287-297

Collins J.H., Elzinga M. (1975) The primary structure of actin from rabbit skeletal muscle: Completion and analysis of the amino acid sequence. *J. Biol. Chem.* 250: 5915-5919

Collins J.H., Greaser M.L., Potter J.D., Horn M.J. (1977) Determination of the amino acid sequence of troponin-C from rabbit skeletal muscle. *J. Biol. Chem.* 252: 6356-6362

Crick F.H.C. (1953) The packing of alpha-helices: simple coiled coils. *Acta Crystallogr.* 6: 689 - 697

Cummins P., Perry S.V. (1973) The subunits and biological activity of polymorphic forms of tropomyosin. *Biochem J* 133: 765-777

Cummins P., Perry S.V. (1974) Chemical and immunochemical characteristics of tropomyosins from striated and smooth muscles. *Biochem. J.* 141: 43-49

Dabrowska R., Nowak E. and Drabikowski W. (1983) Some functional properties of nonpolymerizable and polymerizable tropomyosin. *J. Muscle Res. Cell Motil.* 4: 143-161

Ebashi S., Kodama A. (1965) A new protein factor promoting aggregation of tropomyosin. *J. Biochem.* 58: 107-108

Feller G., Gerday C. (1997) Psychrophilic enzymes: molecular basis of cold adaptation. *Cell Mol. Life Sci.* 53: 830-841

Flicker P.F., Phillips Jr. G.N., Cohen C. (1982) Troponin and its interactions with tropomyosin. An electron microscope study. *J. Mol. Biol.* 162 (2): 495-501

Fudge K. and Heeley D. H. (2011) 55th Biophysical Society (Baltimore) A mutant of Atlantic salmon fast muscle tropomyosin. *Biophysical J.*

Frye J., Klenchin V.A., Rayment I. (2010) Structure of the tropomyosin overlap complex from chicken smooth muscle: insight into the diversity of N-terminal recognition. *Biochemistry* 49: 4908-4920

Gerday C., Aittaleb M., Arpigny J.L., Baise E., Chessa J.-P., Garsoux G., Petrescu I., Feller G. (1997) Psychrophilic enzymes: A thermodynamic challenge. *Biochim. Biophys. Acta.* 1342 (2): 119-131

Gergely J. (1950) On the relationship between myosin and ATPase. *Fed. Proc.* 9: 170-176

Gianese G., Argos P., Pascarella S. (2001) Structural adaptation of enzymes to low temperatures. *Protein Eng.* 14: 141-148.

Gianese G., Bossa F., Pascarella S. (2002) Comparative structural analysis of psychrophilic and meso- and thermophilic enzymes. *Proteins: Structure, Function and Genetics* 47: 236-249

Goonasekara C.L., Heeley D.H. (2008) Conformational properties of striated muscle

tropomyosins from some salmonid fish. *J. Muscle Res. Cell Motil.* 29: 135-143

Goonasekara C.L., Heeley D.H. (2009) Incorporation of an amino-terminally shortened alpha-tropomyosin into thin filaments. Evidence for a troponin-T binding site at the amino-terminus of alpha-tropomyosin. *Biochemistry* 48: 3538 - 3544

Goonasekara C. L., Gallivan L. J., Jackman D.M. and Heeley D.H. (2007) Some binding properties of Omp T digested muscle tropomyosin. *J. Muscle Res. Cell Motil.* 28: 175 - 182.

Gordon A.M., Homsher E., Regnier M. (2000) Regulation of contraction in striated muscle. *Phys. Rev.* 80: 853-924

Greaser M.L., Gergely J. (1971) Reconstitution of troponin activity from three protein components. *J. Biol. Chem.* 246: 4226-4233

Greaser M.L., Gergely K. (1973) Purification and Properties of the components from troponin. *J. Biol. Chem.* 248: 2125-2133

Greaves R.B., Warwicker J. (2007) Mechanisms for stabilization and the maintenance of solubility in proteins from thermophiles. *BMC Struct. Biol.* 7: 18

Greaves R.B., Warwicker J. (2009) Stability and solubility of proteins from extremophiles. *Biochem. Biophys. Res. Commun.* 380: 581-585

Greenfield N.J., Fasman G.D. (1969) Computed circular dichroism spectra for the evaluation of protein conformation. *Biochemistry* 8: 4108-4116

Greenfield N.J., Hitchcock-DeGregori S. E. (1995) The stability of tropomyosin, a two-stranded coiled-coil protein, is primarily a function of the hydrophobicity of residues at the helix-helix interface. *Biochemistry* 34: 16797 – 16805

Greenfield N.J., Stafford W.F., Hitchcock-DeGregori S.E. (1994) The effect of N-terminal acetylation on the structure of an N-terminal tropomyosin peptide and $\alpha\alpha$ -tropomyosin. *Protein Science* 3: 402-410

Greenfield N.J., Huang Y.J., Swapna G.V.T., Bhattacharya A., Rapp B., Singh A., Montelione G.T., Hitchcock-DeGregori S.E. (2006) Solution NMR structure of the junction between tropomyosin molecules: Implications for actin binding and regulation. *J. Mol. Biol.* 364: 80-96.

Grefrath S.P. and Reynolds J.A. (1974) The Molecular Weight of the Major Glycoprotein from the Human Erythrocyte Membrane. *Proc. Natl. Acad. Sci.* 71: 3913–3916.

Gregorio C.C., Granzier H., Sorimachi H., and Labeit S. (1999) Muscle assembly: A titanic movement? *Curr. Opin. Cell Biol.* 11: 18-25

Gross E. (1967) The cyanogen bromide reaction. *Methods Enzymol.* 11: 238-255.

Hanson J., Lowy J. (1963) The structure of F-actin and of actin filaments isolated from muscle.

J. Mol. Biol. 6: 46-60

Harford J.J., Squire J.M. (1990) "Static and time-resolved X-ray diffraction studies of contracting fish muscle" In 'Molecular mechanisms in muscular contraction' (Ed. Squire,

J.M.) *Macmillan Press*. Pp. 287-320.

Hayley M., Chevaldina T., Mudalige W.A.K.A., Jackman D.M., Dobbin A.D., Heeley D.H.

(2008) Shark skeletal muscle tropomyosin is a phosphoprotein. *J. Muscle Res. Cell Motil.* 29:

101-107

Hayley M., Chevaldina T., Heeley D.H. (2011) Cold adaptation of tropomyosin. *Biochemistry* 50:

6559-6566

Heeley D.H. (1994) Investigation of the effects of phosphorylation of rabbit striated muscle α -tropomyosin and rabbit skeletal muscle troponin-T. *Eur. J. Biochem.* 221: 129-137

Heeley D.H., Hong C. (1994) Isolation and characterization of tropomyosin from fish muscle.

Comp. Biochem. Physiol. 108B: 95-106

Heeley D.H., Moir A.J.G., Perry S.V. (1982) Phosphorylation of tropomyosin during

development in mammalian striated muscle. *FEBS Lett.* 146: 115-118

Heeley D.H., Dhoot G.K., Perry S.V. (1985) Factors determining the subunit composition of tropomyosin in mammalian skeletal muscle. *Biochemical J.* 226: 461-468

Heeley D.H., Golosinska K., Smillie L.B. (1987) The effects of troponin T fragments T1 and T2 on the binding of nonpolymerizable tropomyosin to F-actin in the presence and absence of troponin I and troponin C. *J. Biol. Chem.* 262: 9971-9978

Heeley D.H., Watson M.H., Mak A.S., Dubord P., Smillie L.B. (1989) Effect of phosphorylation on the interaction and functional properties of rabbit striated muscle $\alpha\alpha$ -tropomyosin. *J. Biol. Chem.* 264: 2424-2430

Heeley D.H., Bieger T., Waddleton D.M., Hong C., Jackman D.M., McGowan C., Davidson W.S., Beavis R.C. (1995) Characterisation of fast, slow and cardiac muscle tropomyosins from salmonid fish. *Eur. J. Biochem.* 232: 226-234

Herzberg O., James M. N. (1985). Structure of the calcium regulatory muscle protein troponin-C at 2.8 Å resolution. *Nature.* 313: 653-659

Hitchcock-DeGregori S.E., Heald R.W. (1987) Altered actin and troponin binding of amino-terminal variants of chicken striated muscle α -tropomyosin expressed in *Escherichia coli*. *J. Biol. Chem.* 262: 9730-9735

Hitchcock-DeGregori S.E., Varnell T.A. (1990) Tropomyosin has discrete actin-binding sites with sevenfold and fourteenfold periodicities. *J. Mol. Biol.* 214: 885–896

Hitchcock-DeGregori S.E., Singh A. (2010) What makes tropomyosin an actin binding protein: a perspective. *J. Str. Biol.* 170(2): 319-324

Hodges R.S., Smillie L.B. (1972) Cysteine sequences of rabbit skeletal tropomyosin. *Can. J. Biochem.* 50:330-343

Hogdes R.S., Sodek J., Smillie L.B., Jurasek L. (1972) Tropomyosin: amino acid sequence and coiled coil structure. *Cold Spring Harbor Symp. Quant. Biol.* 37:299-310

Holmes K.C., Popp D., Gebhard W., Kabsch W. (1990) Atomic model of the actin filament *Nature* 347: 44 – 49

Huxley A.F. (1974) Muscular Contraction. *J. Physiol.* 243: 1-43

Huxley H.E. (1963) Electron microscope studies on the structure of natural and synthetic protein filaments from striated muscle. *J. Mol. Biol.* 7: 281–308

Huxley H. E. (1972) Structural changes in actin and myosin containing filaments of vertebrate striated muscle. *Cold Spring Harb. Symp. quant. Biol.* 37: 361 – 376

Huxley H.E. (1969) The mechanism of muscular contraction.

Science 164: 1356 – 1365

Jackman D.M., Waddleton D.M., Younghusband B., and Heeley D.H. (1996) Further characterization of fast, slow, and cardiac muscle tropomyosins from salmonid fish. *Eur. J. Biochem.* 242: 363-371

Jackson P., Amphlett G.N., Perry S.V. (1975) The primary structure of troponin T and the interaction with tropomyosin. *Biochem. J.* 151: 85-97

Johnson F., Smillie L.B. (1975) Rabbit skeletal alpha-tropomyosin chains are in register. *Biochem. Biophys. Res. Commun.* 64: 1316–1322

Johnston I.A. (1980) Specialisation of fish muscle. In: Goldspink D.F. (ed.) Development and specialisations of muscle. *Soc. Exp. Biol. Seminar Series Symp.* 7: 123-148

Johnston I.A., Ward P.S., Goldspink G. (1975) Studies on the swimming musculature of the rainbow trout I. Fibre types. *J. Fish Biol.* 7: 451-458

Kabsch W., Mannherz H.G., Suck D., Pai E.F., Holmes K.C. (1990) Atomic structure of the actin:DNase I complex. *Nature.* 347(6288): 37–44

King A.M., Loiselle D.S., and Kohl P. (2004) Force generation for locomotion of vertebrates: Skeletal muscle overview. *IEEE J. Ocean. Eng.* 29(3): 684-691

Laemmli U.K. (1970) Cleavage of structural proteins during the assembly of the head of bacteriophage T4. *Nature* 227: 680-685

Lees-Miller J.P., Helfman D.M. (1991) The molecular basis for tropomyosin isoform diversity. *Bioessays* 13: 429-437

Lehrer S.S. (1975) Intramolecular crosslinking of tropomyosin via disulfide bond formation: evidence for chain register. *Proc. Nat. Acad. Sci., U.S.A.* 72: 3377-3381

Lieber R.L. (2002) Skeletal Muscle Structure, Function, and Plasticity. 2nd ed. Baltimore: Lippincott Williams, and Williams.

Mak A.S., Smillie L.B. (1981) Structural interpretation of the two-site binding of troponin on the muscle thin filament. *J. Mol. Biol.* 149: 541-550

Mak A.S., Smillie L.B., Barany M. (1978) Specific phosphorylation at serine-283 of α -tropomyosin from frog skeletal and rabbit skeletal and cardiac muscle. *Proc. Natl. Acad. Sci. U.S.A.* 75: 3588-359

Mak A.S., Smillie L.B., Stewart G.R. (1980) A comparison of the amino acid sequences of rabbit

skeletal muscle α - and β -tropomyosins. *J. Biol. Chem.* 255: 3647-3655

Mak A.S., Golosinska K., Smilie L.B. (1983) Induction of nonpolymerizable tropomyosin binding to F-actin by troponin and its components. *J. Biol. Chem.* 258: 14330–14334

McLachlan A.D., Stewart M. (1975) Tropomyosin coiled-coil interactions: Evidence for an unstaggered structure. *J. Mol. Biol.* 98: 293-304

Montarass D., Fiszman M.Y., Gros F. (1981) Characterisation of the tropomyosin present in various chick embryo muscle types and in muscle cells differentiated *in vitro*. *J. Biol. Chem.* 256: 4081-4086

Monteiro P.B., Lataro R.C., Ferro J.A. and Reinach F. de C. (1994). Functional alpha-tropomyosin produced in *Escherichia coli*. A dipeptide extension can substitute the amino-terminal acetyl group. *J. Biol. Chem.* 269: 10461 – 10466

Morris E. P., Lehrer S. S. (1984) Troponin-tropomyosin interactions. Fluorescence studies of the binding of troponin, troponin T, and chymotryptic troponin T fragments to specifically labelled tropomyosin. *Biochemistry* 23: 2214–2220

Ohtsuki I. (1979) Molecular arrangement of troponin-T in the thin filament. *J. Biochem.* 86:491-497

Otterbein L.R., Graceffa P., Dominguez R. (2001) The crystal structure of uncomplexed actin in the ADP state. *Science* 293: 708–711

Palm, T., Greenfield N.J., Hitchcock-DeGregori S. E. (2003). Tropomyosin ends determine the stability and functionality of overlap and troponin-T complexes. *Biophys. J* 84, 3181-3189.

Parry D.A.D. (1974) Structural studies on the tropomyosin/troponin complex of vertebrate skeletal muscle. *Biochem. Biophys. Res. Commun.* 57: 216-224

Parry D.A.D. (1981) Analysis of the amino acid sequence of a tropomyosin-binding fragment from troponin-T. *J. Mol. Biol.* 146: 259-263

Pato M.D., Smillie L.B. (1981) Fragments of rabbit striated muscle α -tropomyosin: Preparation of fragments. *J. Biol. Chem.* 256: 593-601

Pato M. D., Mak A.S., Smillie, L. B. (1981) Fragments of rabbit striated muscle α -tropomyosin: Binding to troponin-T. *J. Biol. Chem.* 256: 602-607

Pearlstone J. R., Smillie L. B. (1977) The binding site of rabbit skeletal α -tropomyosin on troponin-T. *Can. J. Biochem.* 55: 1032-1038

Pearlstone J. R., Smillie L. B. (1978) Troponin T fragments: Physical properties and binding to troponin C. *Can. J. Biochem.* 56: 521-527

Pearlstone J.R., Smillie L.B. (1982) Binding of troponin-T fragments to several types of tropomyosin. *J. Biol. Chem.* 257: 10587-10592

Pearlstone J.R., Carpenter M.R., Smillie L.B. (1977a) Primary structure of rabbit skeletal muscle troponin-T: Purification of cyanogen bromide fragments and the amino acid sequence of fragment CB2. *J. Biol. Chem.* 252: 971-977

Pearlstone J.R., Johnson P., Carpenter M.R., Smillie L.B. (1977b) Primary structure of rabbit skeletal muscle troponin-T: Sequence determination of the NH₂-terminal fragment CB3 and the complete sequence of troponin-T. *J. Biol. Chem.* 252: 983-989

Perry S.V. (1951) The adenosinetriphosphatase activity of myofibrils isolated from skeletal muscle. *Biochem. J.* 48:257-265

Perry S.V. (2001) Vertebrate tropomyosin: distribution, properties and function. *J. Muscle Res. Cell Motil.* 22:5-49

Phillips G.N. Jr., Fillers J.P., Cohen C. (1980) Motions of tropomyosin. *Biophys. J.* 32: 485-502

Potter, J. D. (1974) The content of troponin, tropomyosin, actin and myosin in rabbit skeletal

muscle fibrils. *Arch. Biochem. Biophys.* 162: 436-441

Rath A., Glibowicka M., Nadeau V.G., Chen G., Deber C.M. (2009) Detergent binding explains anomalous SDS-PAGE migration of membrane proteins. *Proc. Natl. Acad. Sci.* 106: 1760-1765.

Reynolds J.A., Tanford C. (1970) Binding of Dodecyl Sulfate to Proteins at High Binding Ratios: Possible Implications for the State of Proteins in Biological Membranes. *Proc. Natl. Acad. Sci.* 66: 1002-1007.

Ribulow H., Barany M. (1977) Phosphorylation of tropomyosin in live frog muscle. *Arch. Biochem. Biophys.* 179: 718-720

Sanders C., Smillie L. B. (1985) Amino acid sequence of chicken gizzard gamma-tropomyosin. *J. Biol. Chem.* 260: 7264-7275.

Sender P.M. (1971) Muscle fibrils: Solubilization and gel electrophoresis. *FEBS Lett.* 17: 106 – 110.

Singh A., Hitchcock-Degregori S.E. (2003) Local destabilization of the tropomyosin coiled coil gives the molecular flexibility required for actin binding. *Biochemistry* 42(48): 14114-14121

Smillie L.B. (1979) Structure and functions of tropomyosins from muscle and non-muscle sources. *Trends Biochem. Sci.* 4: 151-155

Stewart M., McLachlan A.D. (1975) Fourteen actin-binding sites on tropomyosin. *Nature* 257: 331-333

Stone D., Smillie L.B. (1978) The amino acid sequence of rabbit skeletal α -tropomyosin. *J. Biol. Chem.* 253: 1137-1148

Stone D., Sodek J., Johnson P., Smillie L. B. (1974) Tropomyosin: correlation of amino acid sequence and structure. *FEBS Proc. Meet.* 31: 125-136

Straub F.B. (1942) Actin. *Stud. Inst. Med. Chem. Univ. Szeged* 2: 3-15

Straub F.B. (1943) Actin II. *Stud. Inst. Med. Chem. Univ. Szeged.* 3:23-37

Syska, H., Wilkinson, J.M., Grand, R.J. and Perry, S.V. (1976) The relationship between biological activity and primary structure of troponin I from white skeletal muscle of the rabbit. *Biochem. J.* 153: 375-387.

Takeda S., Yamashita A., Maeda K., Maéda Y. (2003) Structure of the core domain of human cardiac troponin in the Ca²⁺ saturated form. *Nature* 424: 35-41

Talbot J. A., Hodges R. S. (1981) Synthetic studies on the inhibitory region of rabbit skeletal troponin I. Relationship of amino acid sequence to biological activity. *J. Biol. Chem.* 1981 256: 2798-2802

Ueno H., Tawada H. and Ooi T. (1976) Properties of non-polymerizable tropomyosin obtained by carboxypeptidase digestion. *J. Biochem. (Tokyo)* 180: 283-287

Urbancikova M., Hitchcock-DeGregori S.E. (1994) Requirement of amino-terminal modification for striated muscle α -tropomyosin function. *J. Biol. Chem.* 269: 24310-34315

Vinogradova M.V., Stone D.B., Malanina G.G., Karatzaferi C., Cooke R., Mendelson R.A., Fletterick R.J. (2005) Ca^{2+} regulated structural changes in troponin. *Proc. Natl. Acad. Sci.* 102: 5038-5043

Wang K., McClure J., Tu A. (1979) Titin: major myofibrillar components of striated muscle. *Proc. Natl. Acad. Sci. U.S.A.* 76: 3698 – 3702.

Wegner A. (1979) Equilibrium of the actin-tropomyosin interaction. *J. Mol. Biol.* 131(4): 839–853

Whitby F.G., Phillips Jr. G.N. (2000) Crystal structure of tropomyosin at 7 Angstroms resolution. *Proteins* 38: 49-59

White S.P., Cohen C. and Phillips G.N. (1987) Structure of co-crystals of tropomyosin and troponin. *Nature* 325: 826-828.

Wilkinson J.M., Grand R.J. (1975) The amino acid sequence of troponin I from rabbit skeletal muscle. *Biochem. J.* 149: 493-496

Williams D. L. Jr., Swenson C. A. (1981) Tropomyosin stability: assignment of thermally induced conformational transitions to separate regions of the molecule. *Biochemistry*, 20: 3856-3864

Woodrum D.T., Rich S.A., Pollard T.D. (1975) Evidence for biased bidirectional polymerization of actin filaments using heavy meromyosin prepared by an improved method. *J. Cell Biol.* 67: 231-237

Woods E.F. (1967) Molecular weight and subunit structure of tropomyosin B. *J. Biol. Chem.* 242: 2859-2871

Xiao L., Honig B. (1999) Electrostatic Contributions to the Stability of Hyperthermophilic Proteins. *J. Mol. Biol.* 289:1435-1444

Yamashiro S., Speicher K.D., Speicher D.W., Fowler V.M. (2010) Mammalian tropomodulins nucleate actin polymerization via their actin monomer binding and filament pointed end-capping activities. *J. Biol. Chem.* 285: 33265–33280

Yates L. D., Greaser M. L. (1983) Troponin subunit stoichiometry and content in rabbit skeletal muscle and myofibrils. *Biol. Chem.* 258: 5770-5774.

Zot A.S., Potter J.D. (1987) Structural aspects of troponin-tropomyosin regulation of skeletal and muscle contraction. *Ann. Rev. Biophys. Chem.* 16: 535-559

